Atomic Data and Nuclear Data Tables ▮ (▮▮▮▮) ▮▮▮–▮▮▮

Contents lists available at ScienceDirect

Atomic Data and Nuclear Data Tables

journal homepage: www.elsevier.com/locate/adt

Nuclear chiral doublet bands data tables

B.W. Xiong [a], Y.Y. Wang [b,*]

[a] State Key Laboratory of Nuclear Physics and Technology, School of Physics, Peking University, Beijing 100871, China
[b] School of Physics and Nuclear Energy Engineering and International Research Center for Nuclei and Particles in the Cosmos, Beihang University, Beijing 100191, China

ARTICLE INFO

Article history:
Received 13 April 2018
Received in revised form 30 May 2018
Accepted 31 May 2018
Available online xxxx

Keywords:
Chirality
Chiral doublet bands
Multiple chiral doublets
Rotational spectrum
Electromagnetic transition probability

ABSTRACT

Since the prediction of nuclear chirality in 1997, tremendous progresses both theoretically and experimentally have been achieved. Experimentally, 59 chiral doublet bands in 47 chiral nuclei (including 8 nuclei with multiple chiral doublets) have been reported in $A \sim 80$, 100, 130, and 190 mass regions. The spins, parities, energies, ratios of the magnetic dipole transition strengths to the electric quadrupole transition strengths, and related references for these nuclei are compiled and listed. For these nuclei with the magnetic dipole transition strengths and the electric quadrupole transition strengths measured, the corresponding results are given. A brief discussion is provided after the presentation of energy E, energy difference ΔE, energy staggering parameter $S(I)$, rotational frequency ω, kinematic moment of inertia $\mathcal{J}^{(1)}$, dynamic moment of inertia $\mathcal{J}^{(2)}$, and ratio of the magnetic dipole transition strength to the electric quadrupole transition strength $B(M1)/B(E2)$ versus spin I in each mass region.

* Corresponding author.
E-mail address: flyyuan@buaa.edu.cn (Y.Y. Wang).

https://doi.org/10.1016/j.adt.2018.05.002
0092-640X/

Contents

1. Introduction

Chirality commonly exists in nature, such as the macroscopic spirals of snail shells, the microscopic handedness of certain molecules, and human hands [1]. In geometry, a figure is chiral if it cannot be mapped onto its mirror image by rotations and translations alone. In particle physics, chirality is a dynamic property distinguishing between the parallel and anti-parallel orientations of the intrinsic spin with respect to the momentum of the massless particle. In chemistry, the study of chirality is a very active topic appearing in inorganic, organic, physical, biochemistry, and supramolecular chemistry.

The chirality in nuclear physics was originally suggested by Frauendorf and Meng in 1997 [2]. The physics mechanism of nuclear chirality is illustrated in Fig. 1. For a rotational nucleus with specific triaxial deformation, the collective angular momentum favors alignment along the intermediate axis, which in this case has the largest moment of inertia, while the angular momentum vectors of the valence particles (holes) favor alignment along the nuclear short (long) axis. The three mutually perpendicular angular momenta can be arranged to form two systems with opposite chirality, namely left- and right-handedness. These two systems are transformed into each other by the chiral operator which combines time reversal and spatial rotation of 180°, $\chi = \mathcal{TR}(\pi)$. The spontaneous breaking of chiral symmetry thus happens in the body-fixed reference frame. In the laboratory reference frame, with the restoration of chiral symmetry due to quantum tunneling, the so-called chiral doublet bands, i.e., a pair of $\Delta I = 1$ bands (normally near degenerate) with the same parity, are expected to be observed in triaxial nuclei [2,3].

The nuclear chirality, originally suggested in Ref. [2] and vigorously investigated over the past few years from both the theoretical and experimental standpoint, continues to be the subject of intense discussion. The nuclear chirality has become one of the hot topics in current nuclear physics frontiers, as discussed in recent review articles [3–10].

Theoretically, the nuclear chirality is firstly predicted by particle rotor model (PRM) and tilted axis cranking (TAC) approach in a single-j shell [2]. Later on, various approaches have been developed to describe the nuclear chiral doublet bands.

Depending on the number of valence nucleons and the orbits occupied, 1-particle–1-hole PRM [2,11–15], 2-quasiparticles PRM [16–19], and n-particle-n-hole PRM [20–22] have been developed. The varieties of PRM include core quasiparticle coupling model [23–25], interacting boson fermion–fermion model [26–29], the generalized coherent state model [30], the angular momentum projection method [31], and pair truncated shell model [32,33].

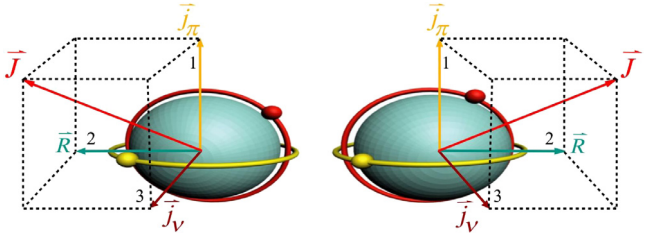

Fig. 1. (Color online) Left- and right-handed chiral systems for a triaxial odd–odd nucleus [3].

The TAC adopted in Ref. [2] is based on a single-j mean field. Combining the spherical Woods–Saxon single-particle energies and the deformed part of the Nilsson potential, chiral rotation has been studied by the Strutinsky shell correction TAC method [34]. More microscopically, TAC based on covariant density functional theory (CDFT) [35,36] has been introduced and applied to the studies of chirality. The self-consistent Skyrme Hartree–Fock cranking model has also been developed [37].

To go beyond mean field approximation to describe the chiral partners, one can incorporate the quantum correlations by means of random phase approximation [38,39] or collective Hamiltonian [40,41]. By taking into account the quantum fluctuation along the collective degree of freedom, the collective Hamiltonian goes beyond the mean field approximation and restores the broken symmetry.

The attempts to understand the chiral doublet bands by the projected shell model (PSM) [42] have been performed in Ref. [43]. Although the observed energy spectra and transitions have been well reproduced in PSM, it is a big challenge to examine the chiral geometry of angular momentum due to the complication that the projected basis is defined in the laboratory frame and forms a nonorthogonal set. Recently, the chiral geometry of the angular momentum is investigated within the framework of PSM. The geometry of the angular momentum is analyzed in terms of the distributions of its components on the three intrinsic axes (*K plot*) as well as the distributions of its tilted angles in the intrinsic frame (*azimuthal plot*) [44,45].

The PRM is a quantal model consisting of the collective rotation and the intrinsic single-particle motions, the energy splitting and quantum tunneling between the doublet bands can be obtained directly. The rigid rotor with quadrupole deformation parameters β and γ is assumed [3].

Starting from an effective nucleon–nucleon interaction with Lorentz invariance, the CDFT naturally includes the spin–orbit

Please cite this article in press as: B.W. Xiong, Y.Y. Wang, Nuclear chiral doublet bands data tables, Atomic Data and Nuclear Data Tables (2018), https://doi.org/10.1016/j.adt.2018.05.002.

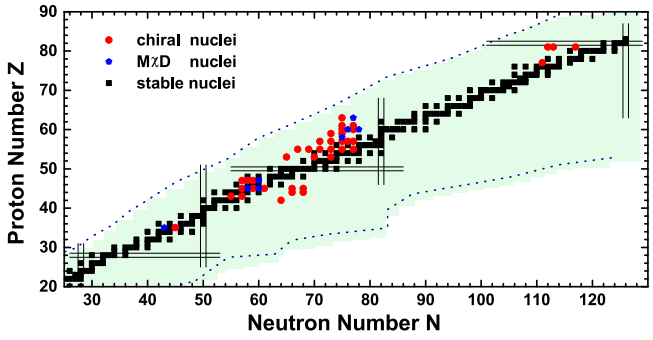

Fig. 2. (Color online) The nuclides with chiral doublet bands (red circles) and MχD (blue pentagons) observed in the nuclear chart. The black squares represent stable nuclides.

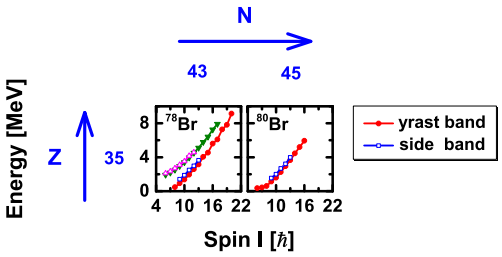

Fig. 3. (Color online) Energies versus spin for chiral doublet bands in $A \sim 80$ mass region. The existence of MχD is suggested in ^{78}Br. The excited chiral doublet bands are shifted by 1.5 MeV.

coupling and has achieved great successes in describing many nuclear phenomena in stable and exotic nuclei of the whole nuclear chart [1,46–49]. It is interesting to search for nuclei with triaxial deformation and configurations having not only one particle and one hole but also several particles and several holes suitable for chirality in CDFT in Ref. [50], the adiabatic and configuration-fixed constrained triaxial CDFT approaches are used to investigate the triaxial shape coexistence and possible chiral doublet bands. A new phenomenon, the existence of multiple chiral doublets (MχD), i.e., more than one pair of chiral doublet bands in one single nucleus, is suggested for ^{106}Rh. This prediction remains with the time-odd fields included [51], and also holds true for other rhodium isotopes [52].

The first experimental evidence for MχD is reported in ^{133}Ce in 2013 [53]. Later, a novel type of MχD with the same configuration is reported in ^{103}Rh [54], which shows that chiral geometry can be robust against the intrinsic excitation. Then, two pairs of positive- and negative-parity doublet bands together with eight strong electric dipole transitions linking their yrast positive- and negative-parity bands, are identified in ^{78}Br. This observation reports the first example of chiral geometry in octupole soft nuclei and indicates that nuclear chirality can be robust against the octupole correlations [55]. Recently, five pairs of nearly degenerate rotational bands were identified in ^{136}Nd [56].

It should be mentioned that two pairs of chiral doublet bands in ^{105}Rh have been independently observed in Refs. [57,58], which have been confirmed to be MχD by adiabatic and configuration-fixed constrained CDFT calculations [59]. Similarly, one pair of chiral doublet bands in ^{107}Ag observed in Ref. [60], which together with nearly degenerate partner bands (though the difference in spin alignment in Fig. 16 needs further clarification) [61], has been claimed to show evidence of MχD [62]. Similarly, for ^{138}Nd, one pair of chiral doublet bands has been suggested in Ref. [63], which together with another pair of partner bands, could be a new candidate of MχD [30].

Generally speaking, for the description of chiral rotations, three dimensional tilted axis cranking CDFT (3D TAC-CDFT) is needed. The 3D TAC-CDFT is firstly developed in Ref. [35]. However, because of its numerical complexity, so far, it has been applied only

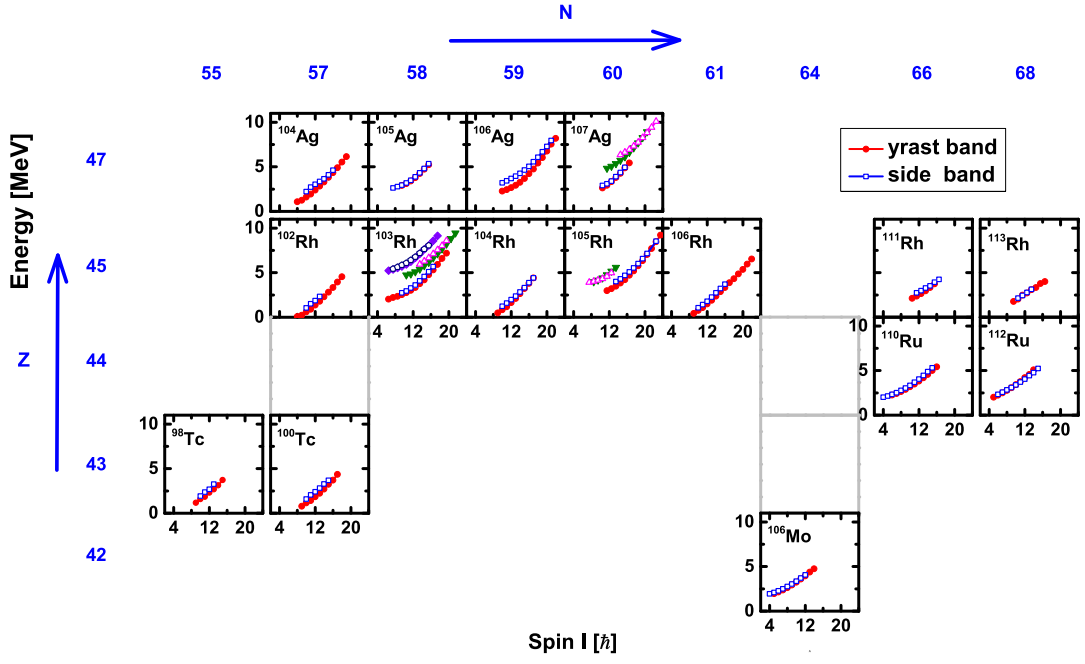

Fig. 4. (Color online) Energies versus spin for chiral doublet bands in $A \sim 100$ mass region. The existence of MχD is suggested in ^{103}Rh, ^{105}Rh, and ^{107}Ag. One pair of excited bands in ^{103}Rh is shifted by 1.5 MeV, and another is shifted by 3 MeV. The excited chiral doublet bands in ^{105}Rh and ^{107}Ag are shifted by 1.5 MeV. The gray boxes are used to connect the various parts of this figure.

Please cite this article in press as: B.W. Xiong, Y.Y. Wang, Nuclear chiral doublet bands data tables, Atomic Data and Nuclear Data Tables (2018), https://doi.org/10.1016/j.adt.2018.05.002.

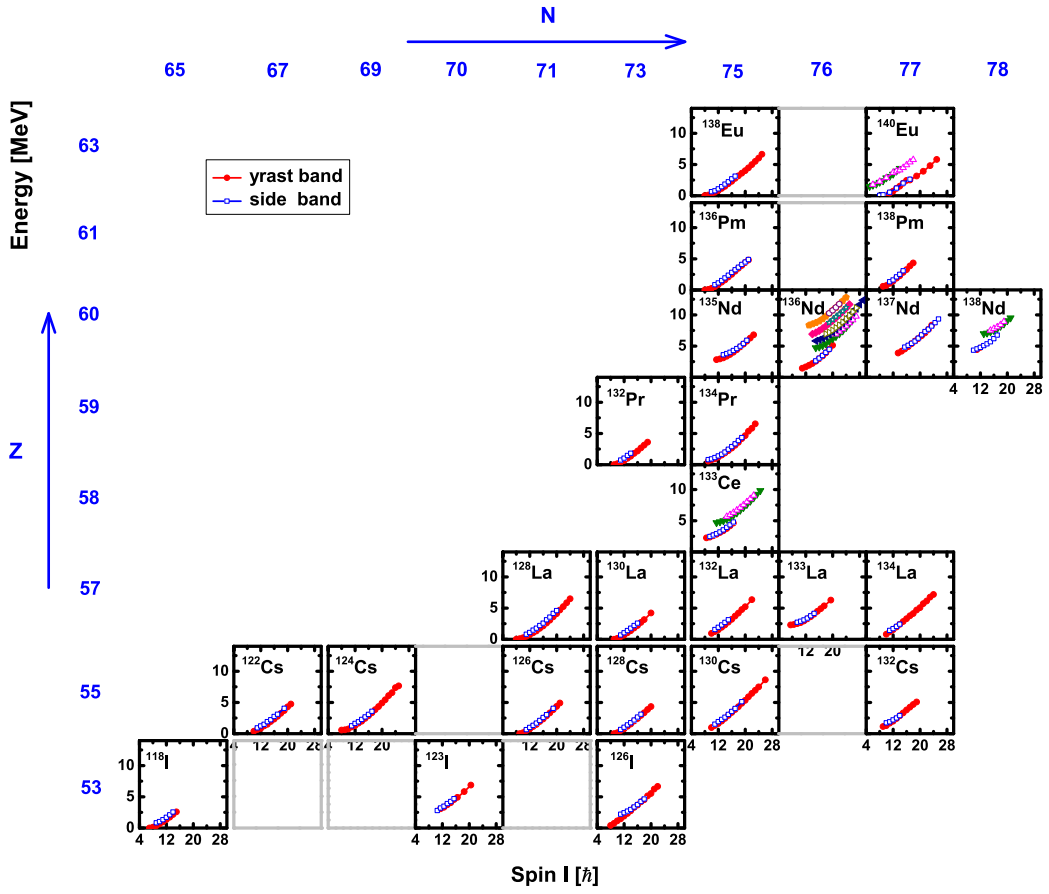

Fig. 5. (Color online) Energies versus spin for chiral doublet bands in $A \sim 130$ mass region. The existences of MχD are suggested in ^{133}Ce,^{136}Nd,^{138}Nd, and ^{140}Eu. For ^{136}Nd, there are five pairs of chiral doublet bands, the two lowest ones are shifted by -3.0 MeV and -1.5 MeV, respectively, and the next two higher ones are shifted by 1.5 MeV and 3.0 MeV, respectively. For other MχD, the excited chiral doublet bands are shifted by 1.5 MeV. The gray boxes are used to connect the various parts of this figure.

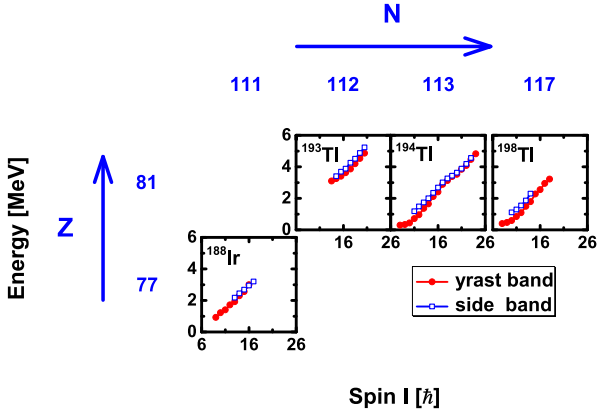

Fig. 6. (Color online) Energies versus spin for chiral doublet bands in $A \sim 190$ mass region.

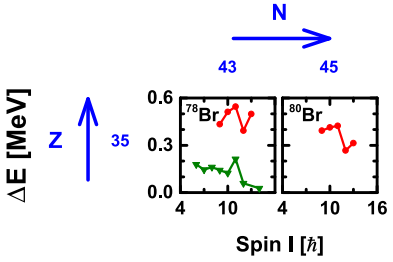

Fig. 7. Energy differences between the chiral doublet bands versus spin in $A \sim 80$ mass region. The red filled circles and olive filled triangles represent the energy differences between the chiral partners and the excited chiral partners, respectively.

for the magnetic rotation in ^{84}Rb. Focusing on the magnetic rotation bands, in 2008, a completely new computer code for the self-consistent 2D TAC-CDFT has been established [64]. It is based on the non-linear meson-exchange models and includes considerable improvements allowing systematic investigations. Based on a point-coupling interaction, the 2D TAC-CDFT is developed to investigated the magnetic rotation bands [65,66], antimagnetic rotation bands [67,68], transitions of nuclear spin orientation [69,70], and linear alpha cluster bands [71], and demonstrates high predictive power [6,36]. Recently, the first applications of the 3D TAC-CDFT for nuclear chirality is reported in ^{106}Rh [72] and ^{136}Nd [56], respectively.

Originally the observation of two almost degenerate $\Delta I = 1$ rotational bands is considered as the fingerprint of chiral doublet bands [2]. With the improvement of experimental techniques, the lifetime measurements for chiral doublet bands become possible. According to the selection rule for the electromagnetic transition in ideal case, there occurs an alternation of stronger and weaker $M1$ transitions with spin over the degenerate spin range of chiral doublet bands, which can manifest as $B(M1)/B(E2)$ staggering as

Please cite this article in press as: B.W. Xiong, Y.Y. Wang, Nuclear chiral doublet bands data tables, Atomic Data and Nuclear Data Tables (2018), https://doi.org/10.1016/j.adt.2018.05.002.

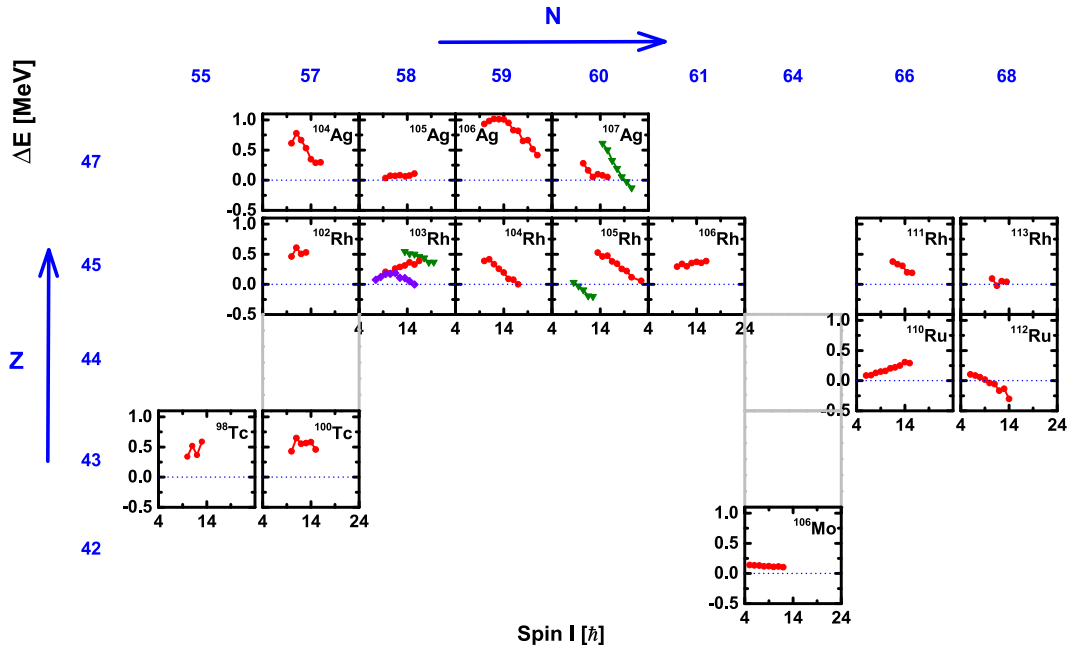

Fig. 8. (Color online) Energy differences between the chiral doublet bands versus spin in $A \sim 100$ mass region.

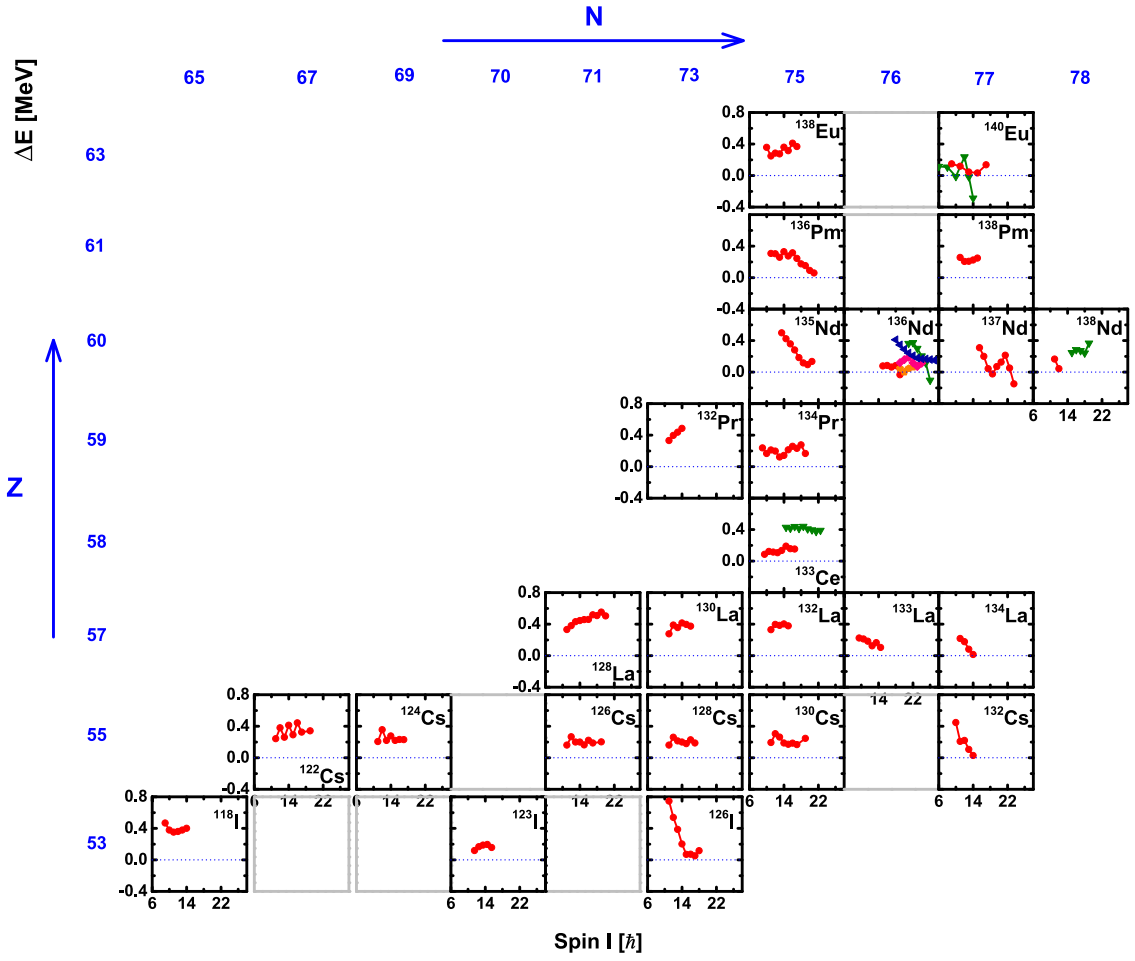

Fig. 9. (Color online) Energy differences between the chiral doublet bands versus spin in $A \sim 130$ mass region.

Please cite this article in press as: B.W. Xiong, Y.Y. Wang, Nuclear chiral doublet bands data tables, Atomic Data and Nuclear Data Tables (2018), https://doi.org/10.1016/j.adt.2018.05.002.

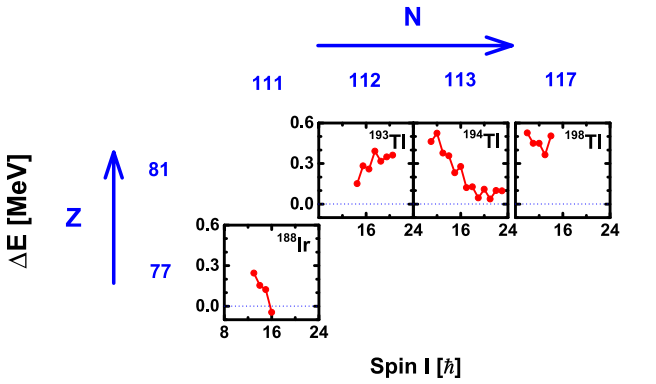

Fig. 10. (Color online) Energy differences between the chiral doublet bands versus spin in $A \sim 190$ mass region.

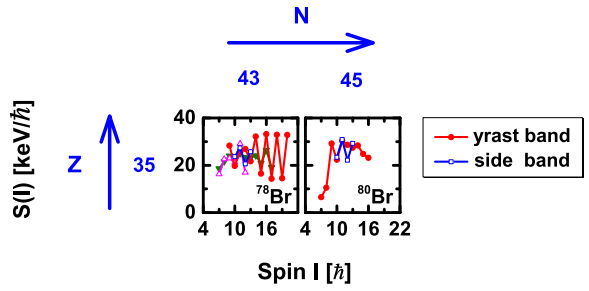

Fig. 11. (Color online) Energy staggering parameters as functions of spin in $A \sim 80$ mass region.

a function of spin I. These characteristics are suggested as electromagnetic transition fingerprints of chiral geometry in Ref. [12]. It is pointed out that in ideal chiral doublet bands, the corresponding properties such as the identical or similarity in energies, spin alignments, and electromagnetic transition probabilities, the spin independence of the energy staggering parameters $S(I)$, and the staggering of $B(M1)/B(E2)$ are summarized as fingerprints of ideal chiral doublet bands [73].

During the last two decades, lots of experimental efforts have been devoted to search for nuclear chirality. Up to now, 59 chiral doublet bands in 47 chiral nuclei (including 8 MχD nuclei) have been reported in the $A \sim 80$ [55,74], 100 [54,57,58,60,75–85], 130 [38,53,56,63,86–105], and 190 [106–109] mass regions. The distribution of the observed chiral nuclei in the nuclear chart is given in Fig. 2.

It should be pointed out that the lifetime measurements which are essential to extract the absolute electromagnetic transition probabilities are still rare for the chiral nuclei candidates.

In order to promote the study of chiral symmetry in atomic nuclei, the compilations of the data for chiral doublet bands are highly demanded. This is the purpose of the present paper.

In Section 2, the figures are presented for energy E, energy difference ΔE, energy staggering parameter $S(I)$, rotational frequency ω, kinematic moment of inertia $\mathcal{J}^{(1)}$, dynamic moment of inertia $\mathcal{J}^{(2)}$, and ratio of the magnetic dipole transition strength to the electric quadrupole transition strength $B(M1)/B(E2)$ versus spin I in each mass region. The explanation of the tables for chiral doublet bands is followed. Finally, a brief summary is given.

2. Systematics of chiral doublet bands

2.1. Energy spectra

The energy spectra for all chiral doublet bands in $A \sim 80$, 100, 130, and 190 mass regions are given in Figs. 3–6, respectively. For MχD in ^{78}Br,^{105}Rh,^{107}Ag,^{133}Ce,^{138}Nd, and ^{140}Eu, the excited chiral doublet bands are shifted by 1.5 MeV. For MχD in ^{103}Rh, there are three pairs of chiral doublet bands, one pair of excited bands are shifted by 1.5 MeV, and another are shifted by 3 MeV. As for MχD in ^{136}Nd, there are five pairs of chiral doublet bands, the two lowest ones are shift by -3.0 MeV and -1.5 MeV, respectively, and the next two higher ones are shift by 1.5 MeV and 3.0 MeV, respectively.

The fingerprint for chiral doublet bands in energy, i.e., two almost degenerate $\Delta I = 1$ rotational bands, is demonstrated in the figures.

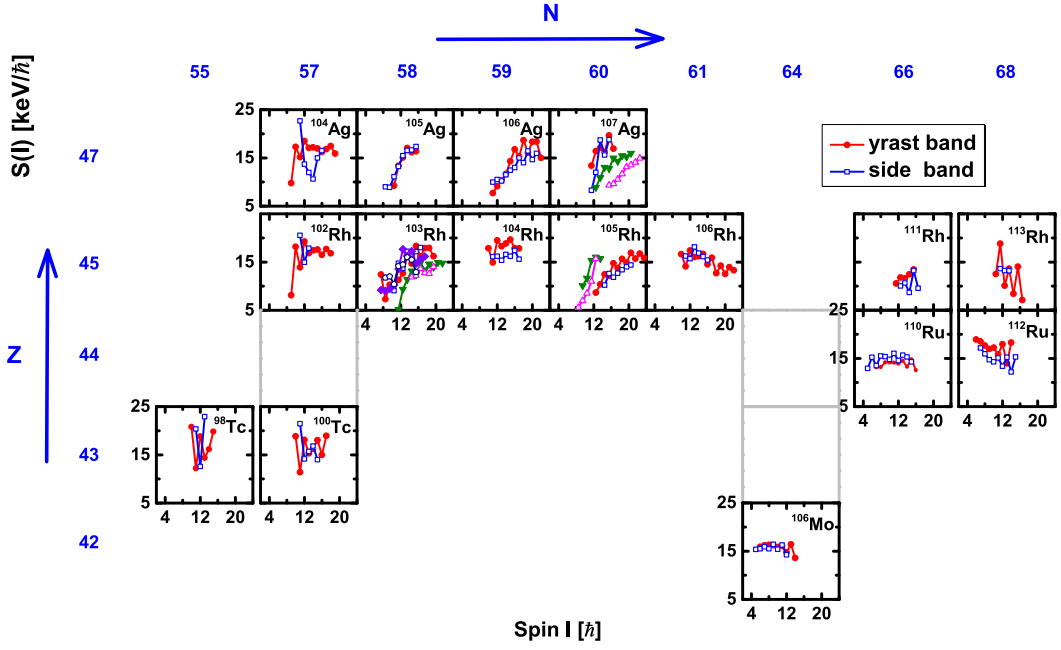

Fig. 12. (Color online) Energy staggering parameters as functions of spin in $A \sim 100$ mass region.

Please cite this article in press as: B.W. Xiong, Y.Y. Wang, Nuclear chiral doublet bands data tables, Atomic Data and Nuclear Data Tables (2018), https://doi.org/10.1016/j.adt.2018.05.002.

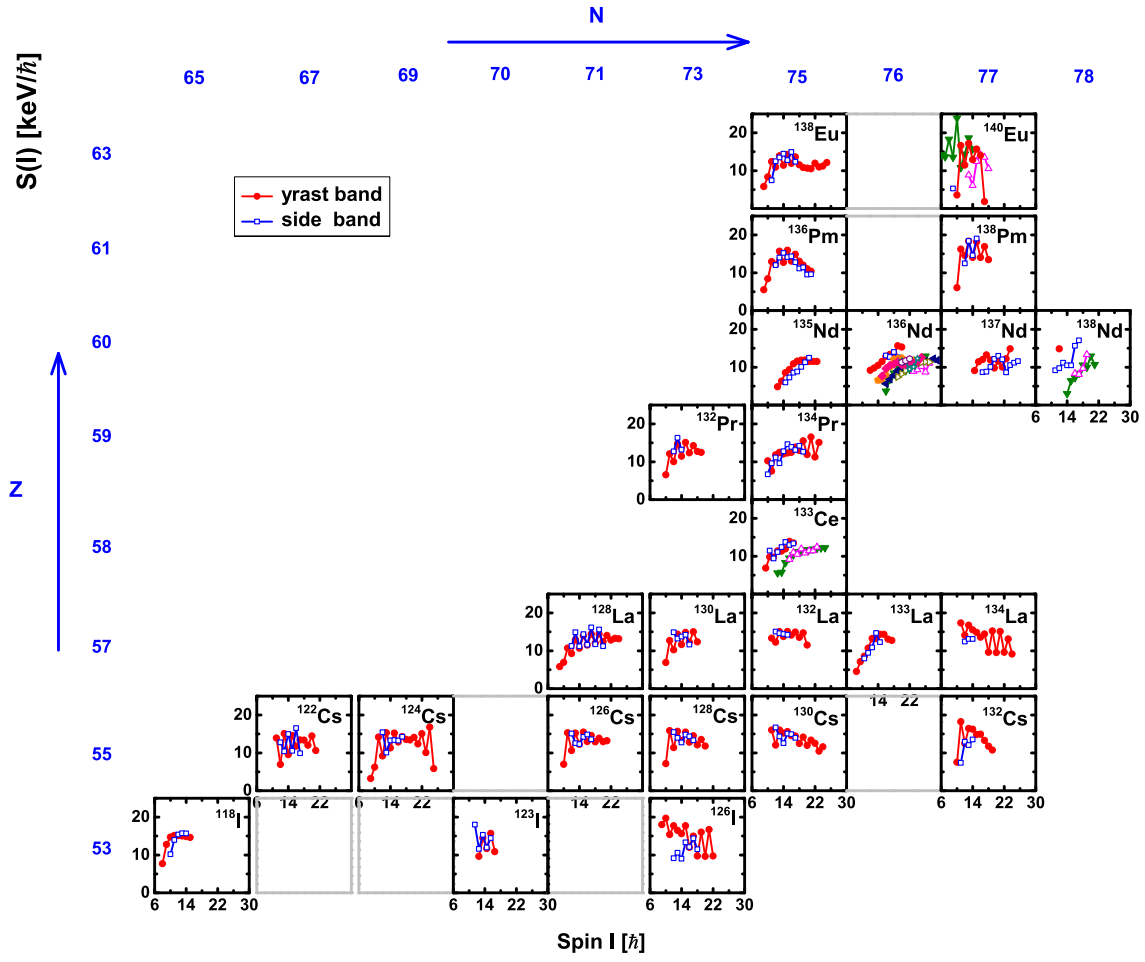

Fig. 13. (Color online) Energy staggering parameters as functions of spin in $A \sim 130$ mass region.

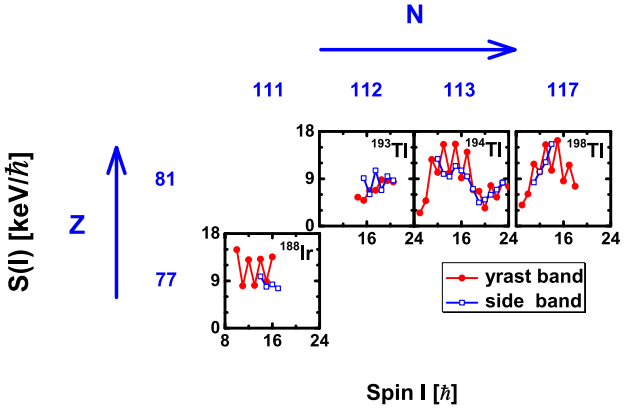

Fig. 14. (Color online) Energy staggering parameters as functions of spin in $A \sim 190$ mass region.

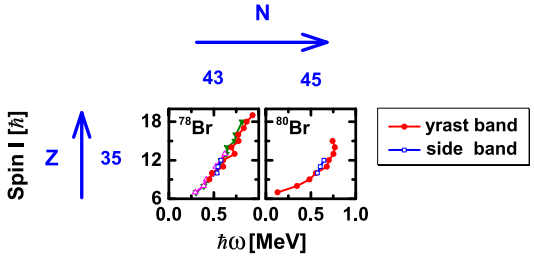

Fig. 15. (Color online) The relation between the spin and the rotational frequency for chiral doublet bands in $A \sim 80$ mass region.

The nuclear chirality occurs at the lowest spin $4\hbar$ in ^{106}Mo and ^{110}Ru, and the highest spin $29\hbar$ in ^{136}Nd. The bands in ^{106}Mo and ^{110}Ru are interpreted as soft chiral vibration [78,110,111]. In ^{136}Nd, the chiral rotations were interpreted by TAC-CDFT with the assigned configurations [56].

Generally, the energies for the partners are close to each other and tend to be almost completely degenerate at high spins. There are several exceptions: for nuclei ^{112}Ru,^{105}Rh,^{107}Ag,^{136}Nd,^{137}Nd, ^{140}Eu, and ^{188}Ir, crossings between some partner bands exist.

2.2. Energy difference

The energy differences $\Delta E(I) = E_{\text{side}}(I) - E_{\text{yrast}}(I)$ between yrast band and side band for all chiral doublet bands in $A \sim 80$, 100, 130, and 190 mass regions are given in Figs. 7–10, respectively. Although the chiral partner bands have energies close to each other, it is rare to observe a crossing between them. If crossing occurs, carefully examinations for chirality are necessary, as has been done in ^{106}Ag [85].

Please cite this article in press as: B.W. Xiong, Y.Y. Wang, Nuclear chiral doublet bands data tables, Atomic Data and Nuclear Data Tables (2018), https://doi.org/10.1016/j.adt.2018.05.002.

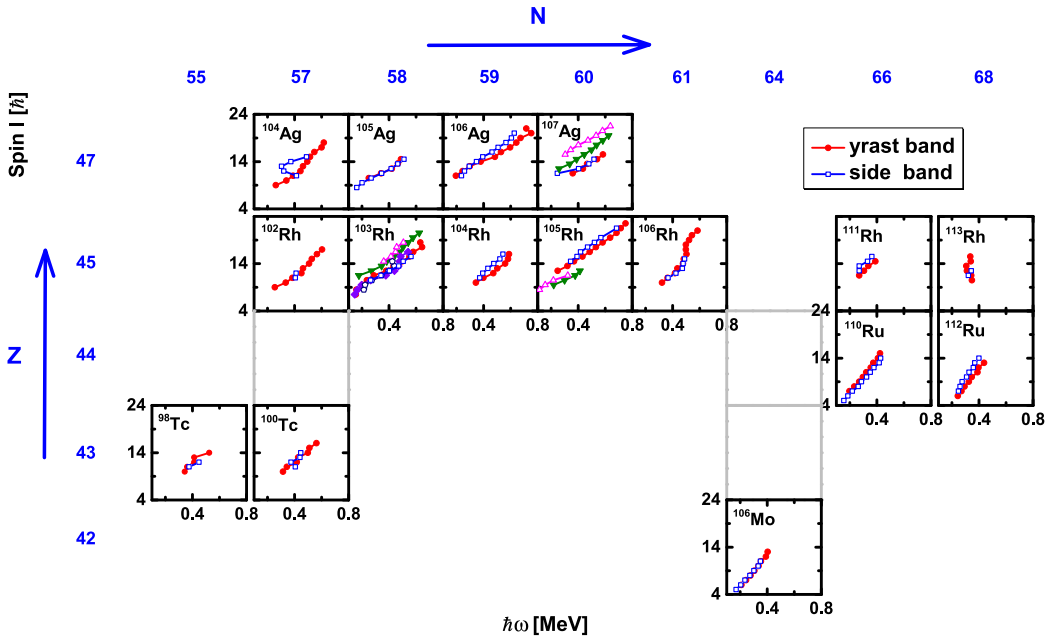

Fig. 16. (Color online) The relation between the spin and the rotational frequency for chiral doublet bands in $A \sim 100$ mass region.

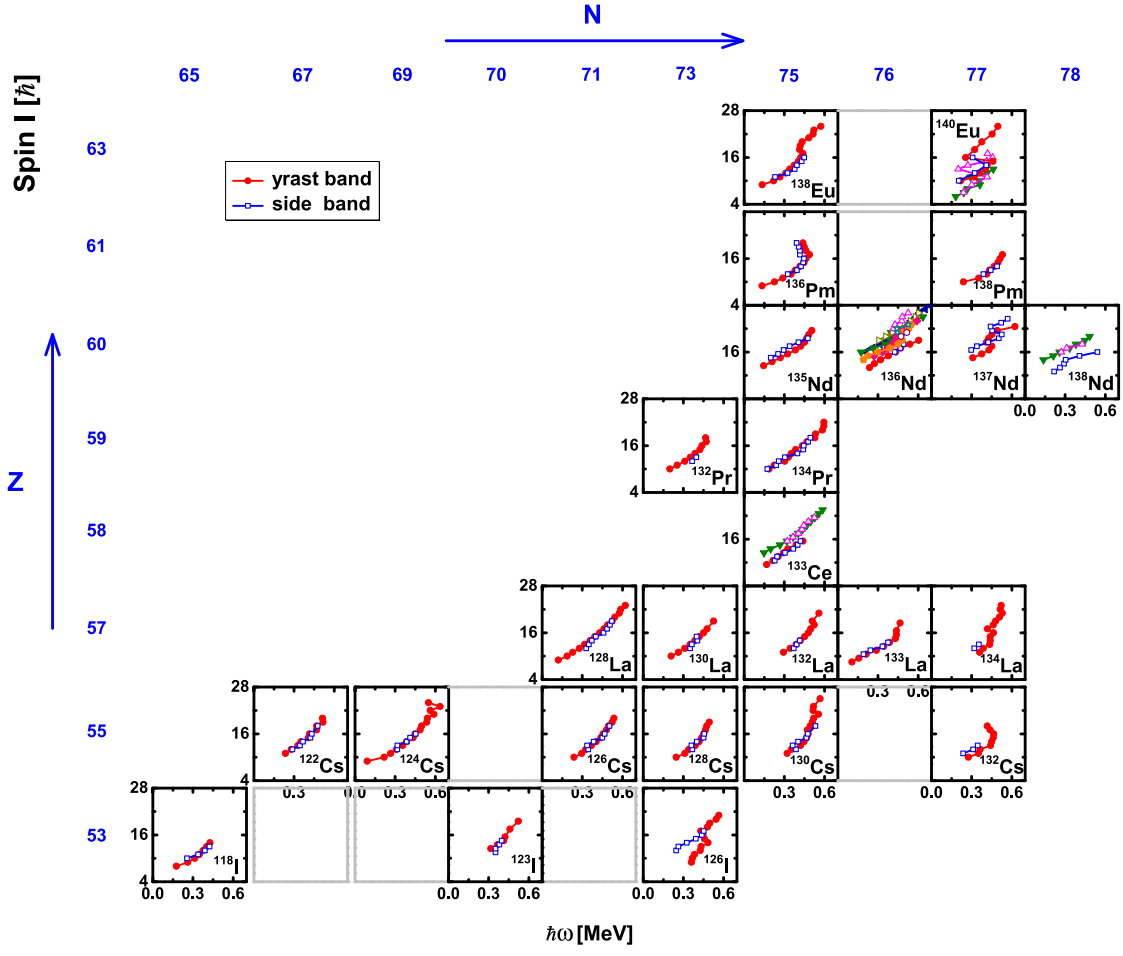

Fig. 17. (Color online) The relation between the spin and the rotational frequency for chiral doublet bands in $A \sim 130$ mass region.

Please cite this article in press as: B.W. Xiong, Y.Y. Wang, Nuclear chiral doublet bands data tables, Atomic Data and Nuclear Data Tables (2018), https://doi.org/10.1016/j.adt.2018.05.002.

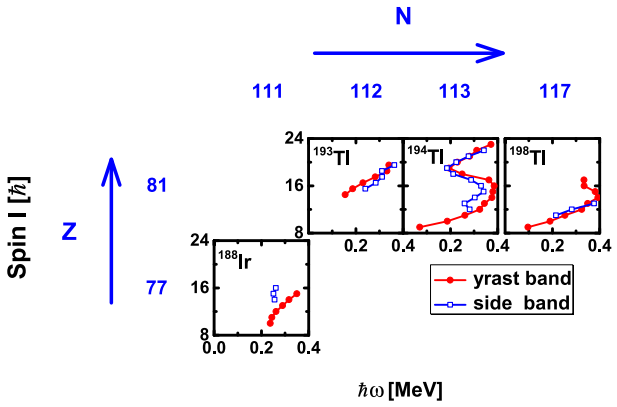

Fig. 18. (Color online) The relation between the spin and the rotational frequency for chiral doublet bands in $A \sim 190$ mass region.

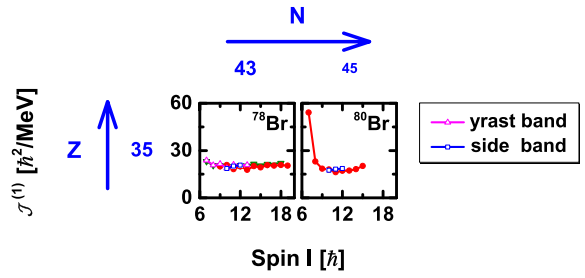

Fig. 19. (Color online) Kinematic moments of inertia versus spin for chiral doublet bands in $A \sim 80$ mass region.

The energy differences ΔE are below 600 keV for all chiral doublet bands except for ^{100}Tc,^{102}Rh,^{104}Ag,^{106}Ag,^{107}Ag, and ^{126}I. Several negative values exist for ΔE in nuclei^{112}Ru,^{105}Rh,^{107}Ag,^{136}Nd, ^{137}Nd,^{140}Eu, and^{188}Ir which correspond to the crossing between the partner bands in Section 2.1.

2.3. Energy staggering

From the energy staggering parameter defined as $S(I) = [E(I) - E(I-1)]/2I$, the energy staggering parameters as functions of spin for all chiral doublet bands in $A \sim 80$, 100, 130, and 190 mass regions are given in Figs. 11–14, respectively.

For the ideal chiral doublet bands, the $S(I)$ values should possess a smooth dependence with spin, and it has been taken as a possible fingerprint.

Normally, the values of $S(I)$ change dramatically at the band head. At certain spin range, they show a smooth dependence with spin. The change of $S(I)$ values is around 20 keV/$\hbar$ in $A \sim 80$ mass region, and decrease to 10 keV/$\hbar$ for most nuclei in $A \sim 100$, 130, and 190 mass regions, except for ^{140}Eu,^{194}Tl, and ^{198}Tl whose change is around 20 keV/$\hbar$.

2.4. Rotational frequency

In order to obtain the response of angular momentum alignments to rotation frequencies and examine the similarities of the configurations for chiral partner bands, the $I - \hbar\omega$ relation has been extracted. From the rotational frequency $\hbar\omega$ defined as [112], $\hbar\omega(I) = [E(I+1) - E(I-1)]/2$, the relations between the spins and the rotational frequencies for all chiral doublet bands in $A \sim 80$, 100, 130, and 190 mass regions are shown in Figs. 15–18, respectively.

Generally, the $I - \hbar\omega$ relation for yrast band and side band is similar, except for ^{104}Ag,^{107}Ag,^{126}I,^{136}Nd,^{137}Nd,^{188}Ir, and ^{193}Tl. Possible backbending in some nuclei exists.

2.5. Kinematic moment of inertia

From the definition $\mathcal{J}^{(1)}(I) = I/\hbar\omega(I)$, the kinematic moments of inertia $\mathcal{J}^{(1)}$ for all chiral doublet bands in $A \sim 80$, 100, 130, and 190 mass regions are shown in Figs. 19–22, respectively.

Generally, the kinematic moment of inertia for yrast band and side band is similar, except for ^{104}Ag,^{107}Ag,^{126}I,^{136}Nd,^{137}Nd,^{140}Eu,

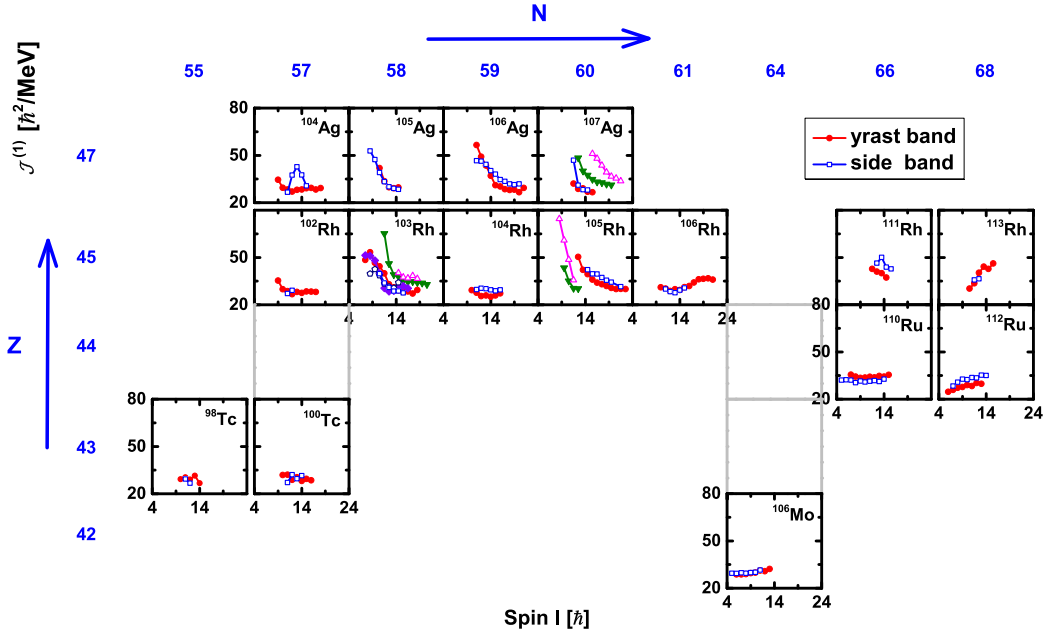

Fig. 20. (Color online) Kinematic moments of inertia versus spin for chiral doublet bands in $A \sim 100$ mass region.

Please cite this article in press as: B.W. Xiong, Y.Y. Wang, Nuclear chiral doublet bands data tables, Atomic Data and Nuclear Data Tables (2018), https://doi.org/10.1016/j.adt.2018.05.002.

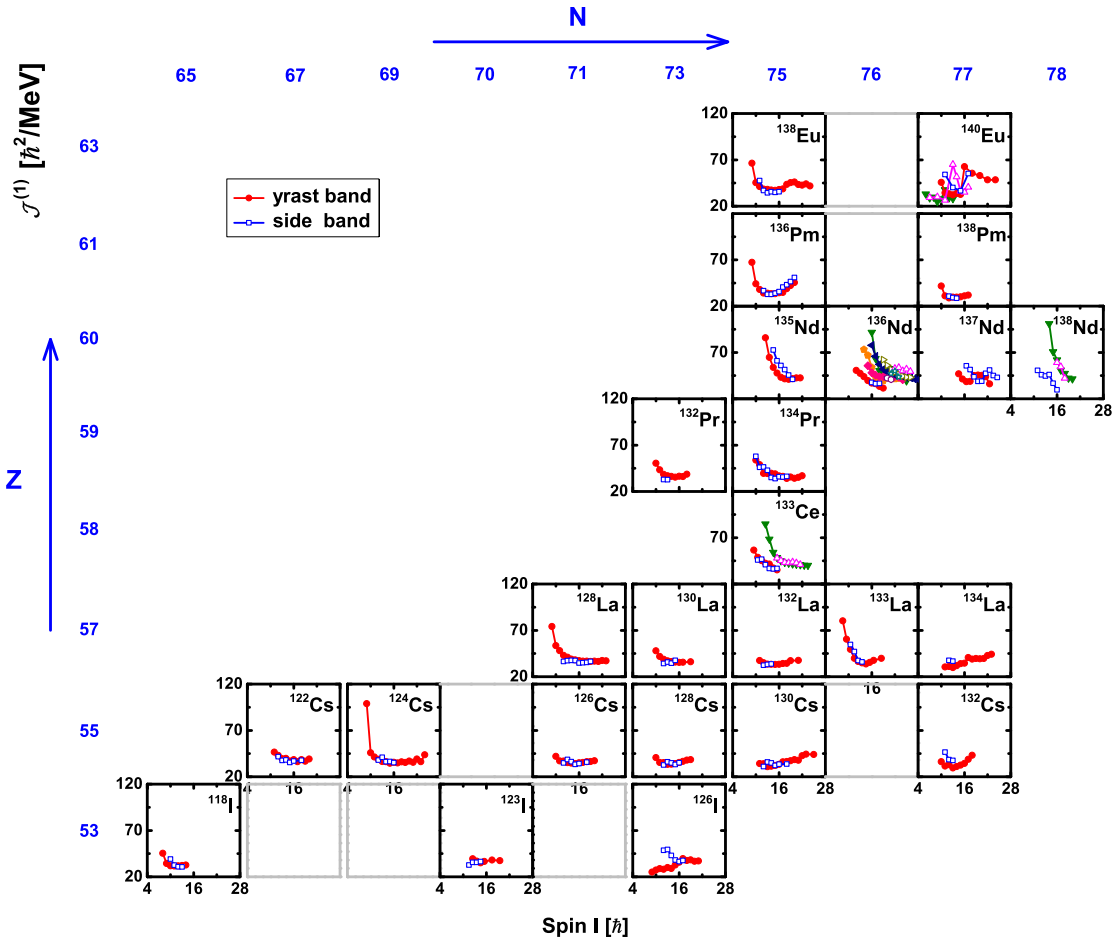

Fig. 21. (Color online) Kinematic moments of inertia versus spin for chiral doublet bands in $A \sim 130$ mass region.

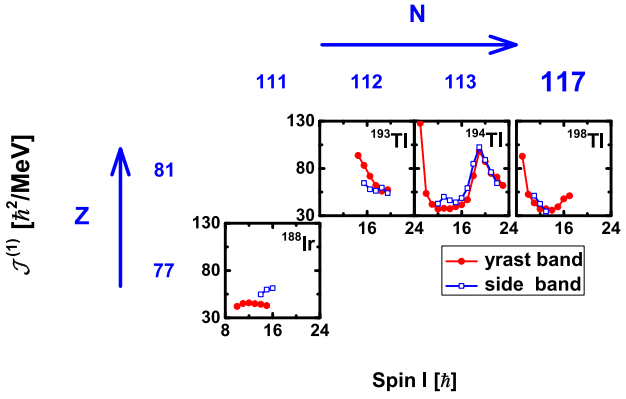

Fig. 22. (Color online) Kinematic moments of inertia versus spin for chiral doublet bands in $A \sim 190$ mass region.

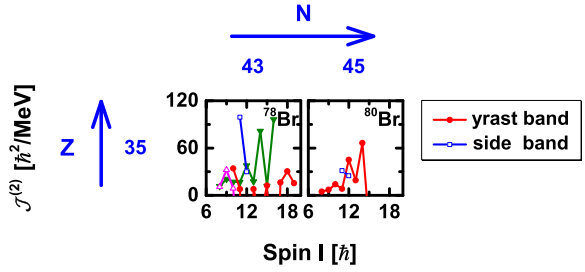

Fig. 23. (Color online) Dynamic moments of inertia versus spin for chiral doublet bands in $A \sim 80$ mass region.

and ^{188}Ir. Normally, the kinematic moment of inertia remains roughly constant.

2.6. Dynamic moment of inertia

From the definition $\mathcal{J}^{(2)}(I) = \hbar\, \mathrm{d}I/\mathrm{d}\omega(I)$, the dynamic moments of inertia $\mathcal{J}^{(2)}$ for all chiral doublet bands in $A \sim 80$, 100, 130, and 190 mass regions are shown in Figs. 23–26, respectively.

Since the $\mathcal{J}^{(2)}$ corresponds to the second derivative of the energy with the spin, a large fluctuation exists. Nevertheless, similarities between the yrast bands and the side bands still exist in most chiral doublet bands.

2.7. Electromagnetic transition probability

The ratios of the magnetic dipole transition strength to the electric quadrupole transition strength $B(M1)/B(E2)$ for all chiral doublet bands in $A \sim 80$, 100, 130, and 190 mass regions are given in Figs. 27–30, respectively. For the ideal chiral bands, due to the restoration of the chiral symmetry in the laboratory frame there are phase consequences for the chiral wavefunctions resulting in

Please cite this article in press as: B.W. Xiong, Y.Y. Wang, Nuclear chiral doublet bands data tables, Atomic Data and Nuclear Data Tables (2018), https://doi.org/10.1016/j.adt.2018.05.002.

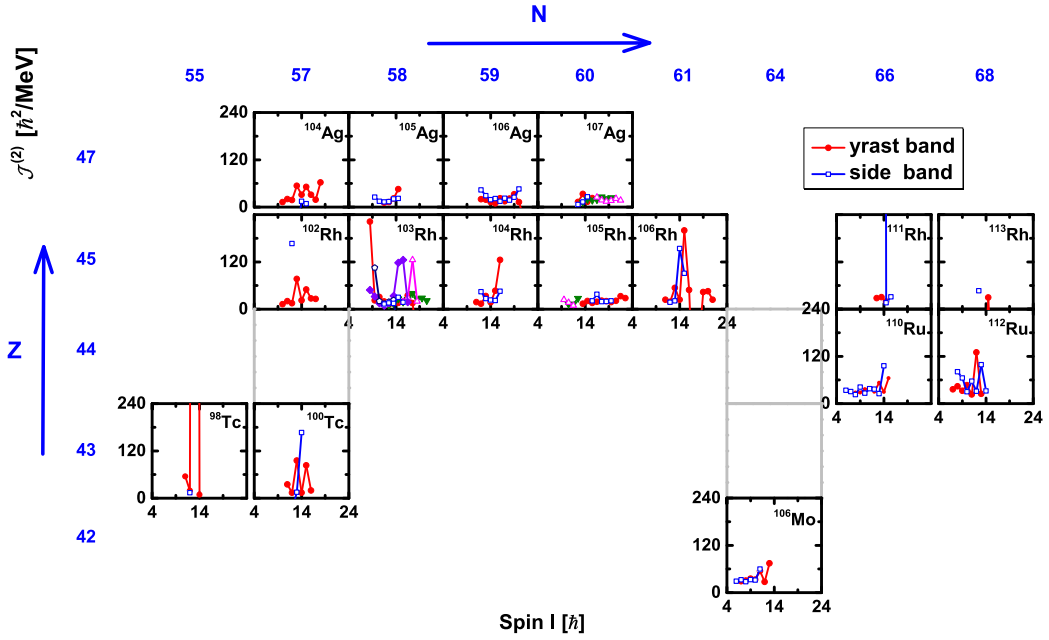

Fig. 24. (Color online) Dynamic moments of inertia versus spin for chiral doublet bands in $A \sim 100$ mass region.

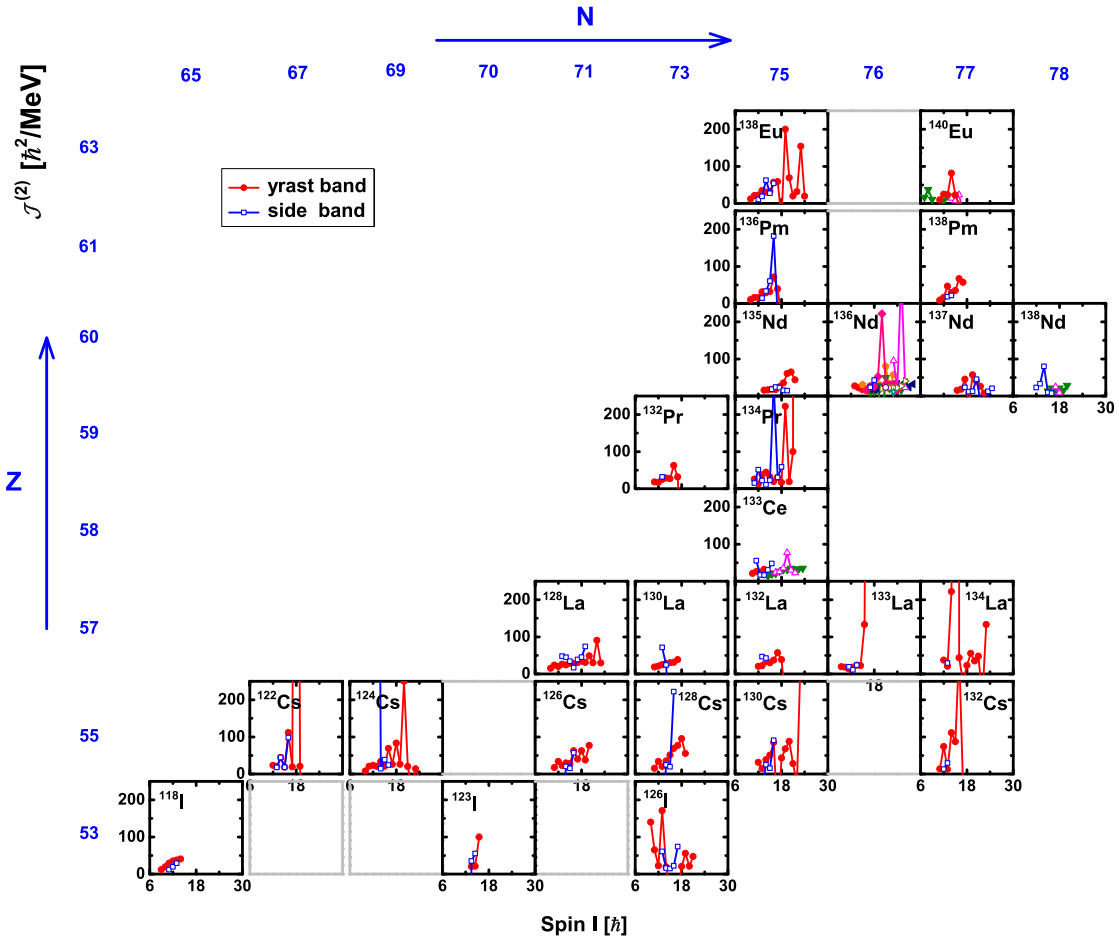

Fig. 25. (Color online) Dynamic moments of inertia versus spin for chiral doublet bands in $A \sim 130$ mass region.

Please cite this article in press as: B.W. Xiong, Y.Y. Wang, Nuclear chiral doublet bands data tables, Atomic Data and Nuclear Data Tables (2018), https://doi.org/10.1016/j.adt.2018.05.002.

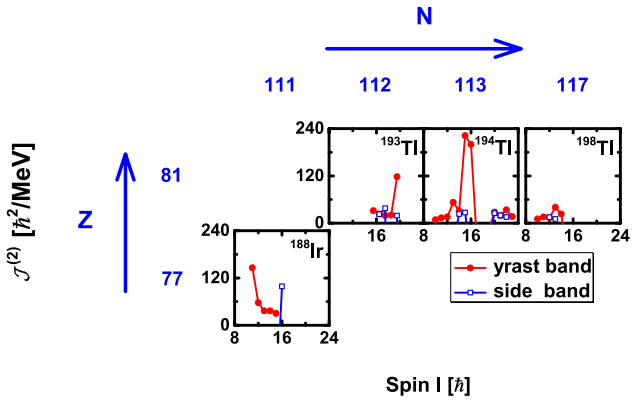

Fig. 26. (Color online) Dynamic moments of inertia versus spin for chiral doublet bands in $A \sim 190$ mass region.

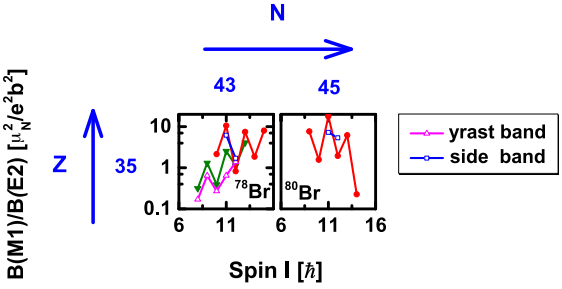

Fig. 27. (Color online) $B(M1)/B(E2)$ ratios versus spin for chiral doublet bands in the $A \sim 80$ mass region.

$M1$ and $E2$ selection rules which can manifest as $B(M1)/B(E2)$ ratios staggering as a function of spin. And the $B(M1)/B(E2)$ ratios are expected to be very similar for the chiral partner bands [73].

For the nuclei ^{106}Mo,^{98}Tc,^{100}Tc,^{110}Ru,^{112}Ru,^{102}Rh,^{106}Rh,^{111}Rh,^{113}Rh,^{104}Ag,^{126}I,^{128}Cs,^{132}Cs,^{132}La,^{134}La,^{134}Pr,^{136}Nd,^{137}Nd,^{138}Nd,^{188}Ir, and ^{198}Tl, the $B(M1)/B(E2)$ ratios are extracted by equation (2) in Ref. [113]. For the nuclei^{104}Rh,^{106}Ag,^{107}Ag,^{124}Cs,^{126}Cs,^{130}Cs,^{135}Nd, and ^{194}Tl with $B(M1)$ and $B(E2)$ values available, the $B(M1)/B(E2)$ ratios are also calculated. The other data available are from the original references. The staggering of the $B(M1)/B(E2)$ ratios exists in most chiral doublet bands.

3. Summary

Since the prediction of nuclear chirality in 1997, the nuclear chirality has become one of the hot topics in current nuclear physics frontiers. Experimentally, 59 chiral doublet bands in 47 chiral nuclei (including 8 nuclei with multiple chiral doublets) have been reported in $A \sim 80$, 100, 130, and 190 mass regions.

The spins, parities, energies, ratios of the magnetic dipole transition strengths to the electric quadrupole transition strengths, and related references for these nuclei have been compiled and listed in Table 1. For these nuclei with the magnetic dipole transition strengths and the electric quadrupole transition strengths measured, the corresponding results have been given in Table 2. A brief discussion has been provided after the presentation of energy E, energy difference ΔE, energy staggering parameter $S(I)$, rotational frequency ω, kinematic moment of inertia $\mathcal{J}^{(1)}$, dynamic moment of inertia $\mathcal{J}^{(2)}$, and ratio of the magnetic dipole transition strength to the electric quadrupole transition strength $B(M1)/B(E2)$ versus spin I in each mass region.

Acknowledgments

The authors are indebted to Prof. J. Meng for the suggestion of this topic and the guidance during this work. The authors express thanks to R. Bark, U. Garg, A. A. Hecht, P. Joshi, T. Koike, C. Liu, M. L. Liu, J. B. Lu, Y. X. Luo, K. Y. Ma, Y. J. Ma, G. Rainovski, A. K. Singh, K. Starosta, J. Timár, B. Wadsworth, S. Y. Wang, Y. Zheng, L. H. Zhu, S. F. Zhu, and S. J. Zhu for providing the data and helpful suggestions. Fruitful discussions with F. Q. Chen, Q. B. Chen, Z. Shi, Y. K. Wang, X. H. Wu, S. Q. Zhang, Z. H. Zhang, and P. W.

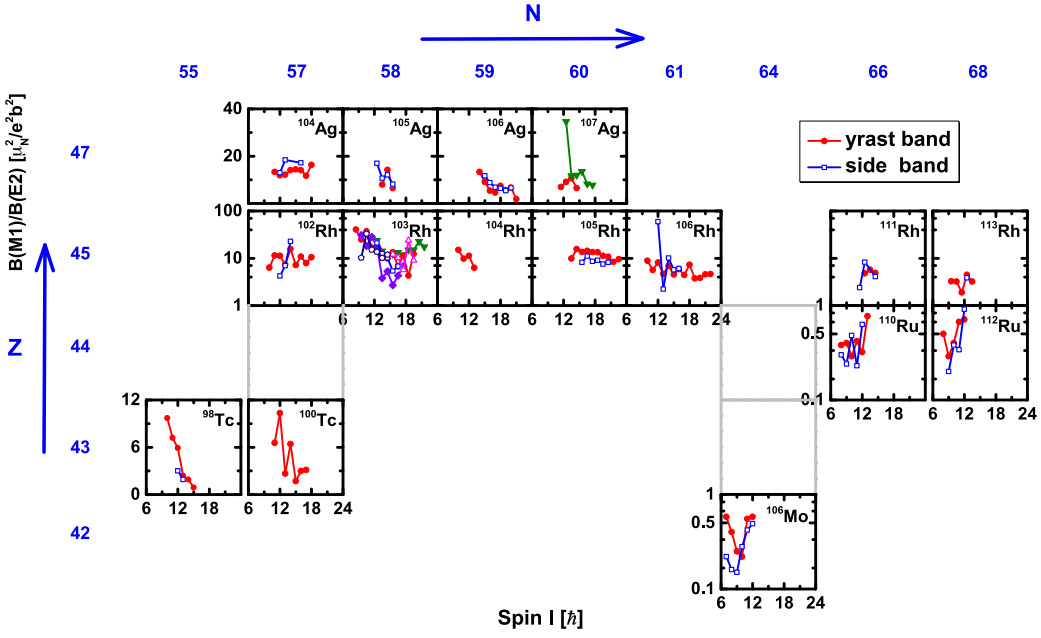

Fig. 28. (Color online) $B(M1)/B(E2)$ ratios versus spin for chiral doublet bands in the $A \sim 100$ mass region.

Please cite this article in press as: B.W. Xiong, Y.Y. Wang, Nuclear chiral doublet bands data tables, Atomic Data and Nuclear Data Tables (2018), https://doi.org/10.1016/j.adt.2018.05.002.

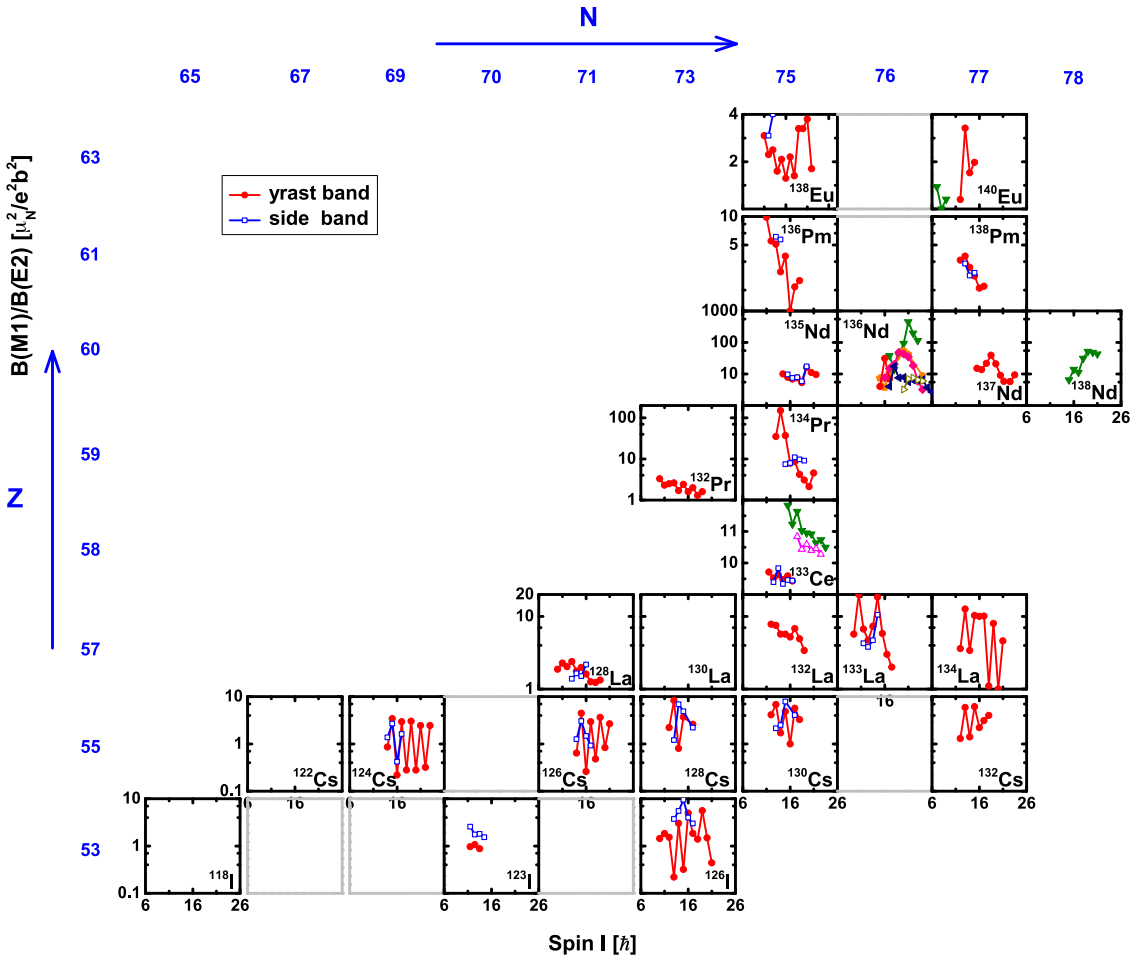

Fig. 29. (Color online) $B(M1)/B(E2)$ ratios versus spin for chiral doublet bands in the $A \sim 130$ mass region.

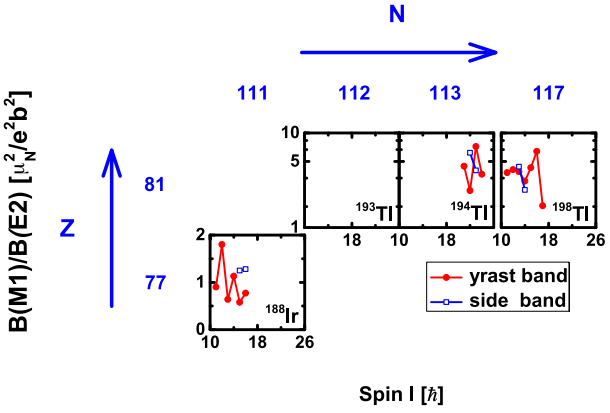

Fig. 30. (Color online) $B(M1)/B(E2)$ ratios versus spin for chiral doublet bands in the $A \sim 190$ mass region.

Zhao are very much appreciated. This work is supported in part by the Major State 973 Program of China (Grant No. 2013CB834400) and the National Natural Science Foundation of China (Grant Nos. 11335002, 11375015, 11461141002, and 11621131001).

References

[1] J. Meng (Ed.), Relativistic Density Functional for Nuclear Structure, International Review of Nuclear Physics, vol. 10, World Scientific, Singapore, 2016, pp. 387–411.
[2] S. Frauendorf, J. Meng, Nuclear Phys. A 617 (1997) 131.
[3] J. Meng, S.Q. Zhang, J. Phys. G: Nucl. Part. Phys. 37 (2010) 064025.
[4] S. Frauendorf, Rev. Modern Phys. 73 (2001) 463.
[5] J. Meng, Internat. J. Modern Phys. E 20 (2011) 341.
[6] J. Meng, P.W. Zhao, Phys. Scr. 91 (2016) 053008.
[7] S.G. Zhou, Phys. Scr. 91 (2016) 063008.
[8] J.A. Sheikh, G.H. Bhat, W.A. Dar, S. Jehangir, P.A. Ganai, Phys. Scr. 91 (2016) 063015.
[9] A.A. Raduta, Prog. Part. Nucl. Phys. 90 (2016) 241.
[10] K. Starosta, T. Koike, Phys. Scr. 92 (2017) 093002.
[11] J. Peng, J. Meng, S.Q. Zhang, Phys. Rev. C 68 (2003) 044324.
[12] T. Koike, K. Starosta, I. Hamamoto, Phys. Rev. Lett. 93 (2004) 172502.
[13] B. Qi, S.Q. Zhang, S.Y. Wang, J.M. Yao, J. Meng, Phys. Rev. C 79 (2009) 041302(R).
[14] B. Qi, S.Q. Zhang, S.Y. Wang, J. Meng, Chin. Phys. Lett. 27 (2010) 112101.
[15] Q.B. Chen, J.M. Yao, S.Q. Zhang, B. Qi, Phys. Rev. C 82 (2010) 067302.
[16] S.Q. Zhang, B. Qi, S.Y. Wang, J. Meng, Phys. Rev. C 75 (2007) 044307.
[17] S.Y. Wang, S.Q. Zhang, B. Qi, J. Peng, J.M. Yao, J. Meng, Phys. Rev. C 77 (2008) 034314.
[18] S.Y. Wang, B. Qi, D.P. Sun, Phys. Rev. C 82 (2010) 027303.
[19] B. Qi, S.Y. Wang, S.Q. Zhang, Chin. Phys. Lett. 28 (2011) 122101.
[20] B. Qi, S.Q. Zhang, J. Meng, S.Y. Wang, S. Frauendorf, Phys. Lett. B 675 (2009) 175.
[21] B. Qi, S.Q. Zhang, S.Y. Wang, J. Meng, T. Koike, Phys. Rev. C 83 (2011) 034303.
[22] B. Qi, J. Li, S.Y. Wang, J. Zhang, S.Q. Zhang, Chin. Phys. Lett. 29 (2012) 072101.
[23] K. Starosta, C.J. Chiara, D.B. Fossan, T. Koike, T.T.S. Kuo, D.R. LaFosse, S.G. Rohoziński, Ch. Droste, T. Morek, J. Srebrny, Phys. Rev. C 65 (2002) 044328.
[24] T. Koike, K. Starosta, C.J. Chiara, D.B. Fossan, D.R. LaFosse, Phys. Rev. C 67 (2003) 044319.
[25] Ch. Droste, S.G. Rohoziński, K. Starosta, L. Próchniak, E. Grodner, Eur. Phys. J. A 42 (2009) 79.
[26] D. Tonev, G. de Angelis, P. Petkov, A. Dewald, S. Brant, S. Frauendorf, D.L. Balabanski, P. Pejovic, D. Bazzacco, P. Bednarczyk, F. Camera, A. Fitzler, A. Gadea, S. Lenzi, S. Lunardi, N. Marginean, O. Möller, D.R. Napoli, A. Paleni, C.M.

Petrache, G. Prete, K.O. Zell, Y.H. Zhang, Jing-ye Zhang, Q. Zhong, D. Curien, Phys. Rev. Lett. 96 (2006) 052501.
[27] D. Tonev, G. de Angelis, S. Brant, S. Frauendorf, P. Petkov, A. Dewald, F. Dönau, D.L. Balabanski, Q. Zhong, P. Pejovic, D. Bazzacco, P. Bednarczyk, F. Camera, D. Curien, F. Della Vedova, A. Fitzler, A. Gadea, G. Lo Bianco, S. Lenzi, S. Lunardi, N. Marginean, O. Möller, D.R. Napoli, R. Orlandi, E. Sahin, A. Saltarelli, J. Valiente Dobon, K.O. Zell, Jing-ye Zhang, Y.H. Zhang, Phys. Rev. C 76 (2007) 044313.
[28] S. Brant, D. Tonev, G. De Angelis, A. Ventura, Phys. Rev. C 78 (2008) 034301.
[29] S. Brant, C.M. Petrache, Phys. Rev. C 79 (2009) 054326.
[30] A.A. Raduta, Al.H. Raduta, C.M. Petrache, J. Phys. G: Nucl. Part. Phys. 43 (2016) 095107.
[31] M. Shimada, Y. Fujioka, S. Tagami, Y.R. Shimizu, Phys. Rev. C 97 (2018) 024319.
[32] K. Higashiyama, N. Yoshinaga, K. Tanabe, Phys. Rev. C 72 (2005) 024315.
[33] K. Higashiyama, N. Yoshinaga, Phys. Rev. C 88 (2013) 034315.
[34] V.I. Dimitrov, S. Frauendorf, F. Dönau, Phys. Rev. Lett. 84 (2000) 5732.
[35] H. Madokoro, J. Meng, M. Matsuzaki, S. Yamaji, Phys. Rev. C 62 (2000) 061301(R).
[36] J. Meng, J. Peng, S.Q. Zhang, P.W. Zhao, Front. Phys. 8 (2013) 55.
[37] P. Olbratowski, J. Dobaczewski, J. Dudek, W. Płóciennik, Phys. Rev. Lett. 93 (2004) 052501.
[38] S. Mukhopadhyay, D. Almehed, U. Garg, S. Frauendorf, T. Li, P.V. Madhusudhana Rao, X. Wang, S.S. Ghugre, M.P. Carpenter, S. Gros, A. Hecht, R.V.F. Janssens, F.G. Kondev, T. Lauritsen, D. Seweryniak, S. Zhu, Phys. Rev. Lett. 99 (2007) 172501.
[39] D. Almehed, F. Dönau, S. Frauendorf, Phys. Rev. C 83 (2011) 054308.
[40] Q.B. Chen, S.Q. Zhang, P.W. Zhao, R.V. Jolos, J. Meng, Phys. Rev. C 87 (2013) 024314.
[41] Q.B. Chen, S.Q. Zhang, P.W. Zhao, R.V. Jolos, J. Meng, Phys. Rev. C 94 (2016) 044301.
[42] K. Hara, Y. Sun, Internat. J. Modern Phys. E 4 (1995) 637.
[43] G.H. Bhat, R.N. Ali, J.A. Sheikh, R. Palit, Nuclear Phys. A 922 (2014) 150.
[44] F.Q. Chen, Q.B. Chen, Y.A. Luo, J. Meng, S.Q. Zhang, Phys. Rev. C 96 (2017) 051303(R).
[45] F.Q. Chen, J. Meng, Acta Phys. Polon. B 11 (2018) 1001.
[46] P. Ring, Prog. Part. Nucl. Phys. 37 (1996) 193.
[47] J. Meng, H. Toki, S.G. Zhou, S.Q. Zhang, W.H. Long, L.S. Geng, Prog. Part. Nucl. Phys. 57 (2006) 470.
[48] J. Meng, S.G. Zhou, J. Phys. G: Nucl. Part. Phys. 42 (2015) 093101.
[49] H.Z. Liang, J. Meng, S.G. Zhou, Phys. Rep. 570 (2015) 1.
[50] J. Meng, J. Peng, S.Q. Zhang, S.G. Zhou, Phys. Rev. C 73 (2006) 037303.
[51] J.M. Yao, B. Qi, S.Q. Zhang, J. Peng, S.Y. Wang, J. Meng, Phys. Rev. C 79 (2009) 067302.
[52] J. Peng, H. Sagawa, S.Q. Zhang, J.M. Yao, Y. Zhang, J. Meng, Phys. Rev. C 77 (2008) 024309.
[53] A.D. Ayangeakaa, U. Garg, M.D. Anthony, S. Frauendorf, J.T. Matta, B.K. Nayak, D. Patel, Q.B. Chen, S.Q. Zhang, P.W. Zhao, B. Qi, J. Meng, R.V.F. Janssens, M.P. Carpenter, C.J. Chiara, F.G. Kondev, T. Lauritsen, D. Seweryniak, S. Zhu, S.S. Ghugre, R. Palit, Phys. Rev. Lett. 110 (2013) 172504.
[54] I. Kuti, Q.B. Chen, J. Timár, D. Sohler, S.Q. Zhang, Z.H. Zhang, P.W. Zhao, J. Meng, K. Starosta, T. Koike, E.S. Paul, D.B. Fossan, C. Vaman, Phys. Rev. Lett. 113 (2014) 032501.
[55] C. Liu, S.Y. Wang, R.A. Bark, S.Q. Zhang, J. Meng, B. Qi, P. Jones, S.M. Wyngaardt, J. Zhao, C. Xu, S.-G. Zhou, S. Wang, D.P. Sun, L. Liu, Z.Q. Li, N.B. Zhang, H. Jia, X.Q. Li, H. Hua, Q.B. Chen, Z.G. Xiao, H.J. Li, L.H. Zhu, T.D. Bucher, T. Dinoko, J. Easton, K. Juhász, A. Kamblawe, E. Khaleel, N. Khumalo, E.A. Lawrie, J.J. Lawrie, S.N.T. Majola, S.M. Mullins, S. Murray, J. Ndayishimye, D. Negi, S.P. Noncolela, S.S. Ntshangase, B.M. Nyakó, J.N. Orce, P. Papka, J.F. Sharpey-Schafer, O. Shirinda, P. Sithole, M.A. Stankiewicz, M. Wiedeking, Phys. Rev. Lett. 116 (2016) 112501.
[56] C.M. Petrache, B.F. Lv, A. Astier, E. Dupont, Y.K. Wang, S.Q. Zhang, P.W. Zhao, Z.X. Ren, J. Meng, P.T. Greenlees, H. Badran, D.M. Cox, T. Grahn, R. Julin, S. Juutinen, J. Konki, J. Pakarinen, P. Papadakis, J. Partanen, P. Rahkila, M. Sandzelius, J. Saren, C. Scholey, J. Sorri, S. Stolze, J. Uusitalo, B. Cederwall, Ö. Aktas, A. Ertoprak, H. Liu, S. Matta, P. Subramaniam, S. Guo, M.L. Liu, X.H. Zhou, K.L. Wang, I. Kuti, J. Timár, A. Tucholski, J. Srebrny, C. Andreoiu, Phys. Rev. C 97 (2018) 041304(R).
[57] J.A. Alcántara-Núñez, J.R.B. Oliveira, E.W. Cybulska, N.H. Medina, M.N. Rao, R.V. Ribas, M.A. Rizzutto, W.A. Seale, F. Falla-Sotelo, K.T. Wiedemann, V.I. Dimitrov, S. Frauendorf, Phys. Rev. C 69 (2004) 024317.
[58] J. Timár, P. Joshi, K. Starosta, V.I. Dimitrov, D.B. Fossan, J. Molnár, D. Sohler, R. Wadsworth, A. Algora, P. Bednarczyk, D. Curieng, Zs. Dombrádi, G. Duchene, A. Gizon, J. Gizon, D.G. Jenkins, T. Koike, A. Krasznahorkay, E.S. Paul, P.M. Raddon, G. Rainovski, J.N. Scheurer, A.J. Simons, C. Vaman, A.R. Wilkinson, L. Zolnai, S. Frauendorf, Phys. Lett. B 598 (2004) 178.
[59] J. Li, S.Q. Zhang, J. Meng, Phys. Rev. C 83 (2011) 037301.
[60] C.Y. He, B. Zhang, L.H. Zhu, X.G. Wu, H.B. Sun, Y. Zheng, B.B. Yu, L.L. Wang, G.S. Li, S.H. Yao, C. Xu, J.G. Wang, L. Gu, Plasma Sci. Technol. 14 (2012) 518.
[61] Dan Jerrestam, W. Klamra, J. Gizon, F. Lidén, L. Hildingsson, J. Kownacki, Th. Lindblad, J. Nyberg, Nuclear Phys. A 577 (1994) 786.
[62] B. Qi, H. Jia, N.B. Zhang, C. Liu, S.Y. Wang, Phys. Rev. C 88 (2013) 027302.
[63] C.M. Petrache, S. Frauendorf, M. Matsuzaki, R. Leguillon, T. Zerrouki, S. Lunardi, D. Bazzacco, C.A. Ur, E. Farnea, C. Rossi Alvarez, R. Venturelli, G. de Angelis, Phys. Rev. C 86 (2012) 044321.
[64] J. Peng, J. Meng, P. Ring, S.Q. Zhang, Phys. Rev. C 78 (2008) 024313.
[65] P.W. Zhao, S.Q. Zhang, J. Peng, H.Z. Liang, P. Ring, J. Meng, Phys. Lett. B 699 (2011) 181.
[66] L.F. Yu, P.W. Zhao, S.Q. Zhang, P. Ring, J. Meng, Phys. Rev. C 85 (2012) 024318.
[67] P.W. Zhao, J. Peng, H.Z. Liang, P. Ring, J. Meng, Phys. Rev. Lett. 107 (2011) 122501.
[68] P.W. Zhao, J. Peng, H.Z. Liang, P. Ring, J. Meng, Phys. Rev. C 85 (2012) 054310.
[69] P.W. Zhao, S.Q. Zhang, J. Meng, Phys. Rev. C 92 (2015) 034319.
[70] Y.K. Wang, Phys. Rev. C 96 (2017) 054324.
[71] P.W. Zhao, N. Itagaki, J. Meng, Phys. Rev. Lett. 115 (2015) 022501.
[72] P.W. Zhao, Phys. Lett. B 773 (2017) 1.
[73] S.Y. Wang, S.Q. Zhang, B. Qi, J. Meng, Chin. Phys. Lett. 24 (2007) 664.
[74] S.Y. Wang, B. Qi, L. Liu, S.Q. Zhang, H. Hua, X.Q. Li, Y.Y. Chen, L.H. Zhu, J. Meng, S.M. Wyngaardt, P. Papka, T.T. Ibrahim, R.A. Bark, P. Datta, E.A. Lawrie, J.J. Lawrie, S.N.T. Majola, P.L. Masiteng, S.M. Mullins, J. Gál, G. Kalinka, J. Molnár, B.M. Nyakó, J. Timár, K. Juhász, R. Schwengner, Phys. Lett. B 703 (2011) 40.
[75] S.J. Zhu, J.H. Hamilton, A.V. Ramayya, J.K. Hwang, J.O. Rasmussen, Y.X. Luo, K. Li, J.G. Wang, X.L. Che, H.B. Ding, S. Frauendorf, V. Dimitrov, Q. Xu, L. Gu, Y.Y. Yang, Chin. Phys. C 33 (2009) 145.
[76] H.B. Ding, S.J. Zhu, J.G. Wang, L. Gu, Q. Xu, Z.G. Xiao, E.Y. Yeoha, M. Zhang, L.H. Zhu, X.G. Wu, Y. Liu, C.Y. He, L.L. Wang, B. Pan, G.S. Li, Chin. Phys. Lett. 27 (2010) 072501.
[77] P. Joshi, A.R. Wilkinson, T. Koike, D.B. Fossan, S. Finnigan, E.S. Paul, P.M. Raddon, G. Rainovski, K. Starosta, A.J. Simons, C. Vaman, R. Wadsworth, Eur. Phys. J. A 24 (2005) 23.
[78] Y.X. Luo, S.J. Zhu, J.H. Hamilton, A.V. Ramayya, C. Goodin, K. Li, X.L. Che, J.K. Hwang, I.Y. Lee, Z. Jiang, G.M. Ter-akopian, A.V. Daniel, M.A. Stoyer, R. Donangelo, S. Frauendorf, V. Dimitrov, Jing-ye Zhang, J.D. Cole, N.J. Stone, J.O. Rasmussen, Internat. J. Modern Phys. E 18 (2009) 1697.
[79] D. Tonev, M.S. Yavahchova, N. Goutev, G. de Angelis, P. Petkov, R.K. Bhowmik, R.P. Singh, S. Muralithar, N. Madhavan, R. Kumar, M. Kumar Raju, J. Kaur, G. Mohanto, A. Singh, N. Kaur, R. Garg, A. Shukla, Ts.K. Marinov, S. Brant, Phys. Rev. Lett. 112 (2014) 052501.
[80] C. Vaman, D.B. Fossan, T. Koike, K. Starosta, I.Y. Lee, A.O. Macchiavelli, Phys. Rev. Lett. 92 (2004) 032501.
[81] P. Joshi, D.G. Jenkins, P.M. Raddon, A.J. Simons, R. Wadsworth, A.R. Wilkinson, D.B. Fossan, T. Koike, K. Starosta, C. Vaman, J. Timár, Zs. Dombrádi, A. Krasznahorkay, J. Molnár, D. Sohler, L. Zolnai, A. Algora, E.S. Paul, G. Rainovski, A. Gizon, J. Gizon, P. Bednarczyk, D. Curien, G. Duchêne, J.N. Scheurer, Phys. Lett. B 595 (2004) 135.
[82] Y.X. Luo, S.C. Wu, J. Gilat, J.O. Rasmussen, J.H. Hamilton, A.V. Ramayya, J.K. Hwang, C.J. Beyer, S.J. Zhu, J. Kormicki, X.Q. Zhang, E.F. Jones, P.M. Gore, I-Yang Lee, P. Zielinski, C.M. Folden, T.N. Ginter, P. Fallon, G.M. Ter-Akopian, A.V. Daniel, M.A. Stoyer, J.D. Cole, R. Donangelo, S.J. Asztalos, A. Gelberg, Phys. Rev. C 69 (2004) 024315.
[83] Z.G. Wang, M.L. Liu, Y.H. Zhang, X.H. Zhou, B.T. Hu, N.T. Zhang, S. Guo, B. Ding, Y.D. Fang, J.G. Wang, G.S. Li, Y.H. Qiang, S.C. Li, B.S. Gao, Y. Zheng, W. Hua, X.G. Wu, C.Y. He, Y. Zheng, C.B. Li, J.J. Liu, S.P. Hu, Phys. Rev. C 88 (2013) 024306.
[84] J. Timár, T. Koike, N. Pietralla, G. Rainovski, D. Sohler, T. Ahn, G. Berek, A. Costin, K. Dusling, T.C. Li, E.S. Paul, K. Starosta, C. Vaman, Phys. Rev. C 76 (2007) 024307.
[85] E.O. Lieder, R.M. Lieder, R.A. Bark, Q.B. Chen, S.Q. Zhang, J. Meng, E.A. Lawrie, J.J. Lawrie, S.P. Bvumbi, N.Y. Kheswa, S.S. Ntshangase, T.E. Madiba, P.L. Masiteng, S.M. Mullins, S. Murray, P. Papka, D.G. Roux, O. Shirinda, Z.H. Zhang, P.W. Zhao, Z.P. Li, J. Peng, B. Qi, S.Y. Wang, Z.G. Xiao, C. Xu, Phys. Rev. Lett. 112 (2014) 202502.
[86] K. Starosta, T. Koike, C.J. Chiara, D.B. Fossan, D.R. LaFosse, Nuclear Phys. A 682 (2001) 375c.
[87] Y.X. Zhao, T. Komatsubara, Y.J. Ma, Y.H. Zhang, S.Y. Wang, Y.Z. Liu, K. Furuno, Chin. Phys. Lett. 26 (2009) 082301.
[88] Y. Zheng, L.H. Zhu, X.G. Wu, Z.C. Gao, C.Y. He, G.S. Li, L.L. Wang, Y.S. Chen, Y. Sun, X. Hao, Y. Liu, X.Q. Li, B. Pan, Y.J. Ma, Z.Y. Li, H.B. Ding, Phys. Rev. C 86 (2012) 014320.
[89] U. Yon-Nam, S.J. Zhu, M. Sakhaee, L.M. Yang, C.Y. Gan, L.Y. Zhu, R.Q. Xu, X.L. Che, M.L. Li, Y.J. Chen, S.X. Wen, X.G. Wu, L.H. Zhu, G.S. Li, J. Peng, S.Q. Zhang, J. Meng, J. Phys. G: Nucl. Part. Phys. 31 (2005) B1.
[90] K. Selvakumar, A.K. Singh, Chandan Ghosh, Purnima Singh, A. Goswami, R. Raut, A. Mukherjee, U. Datta, P. Datta, S. Roy, G. Gangopadhyay, S. Bhowal,

Please cite this article in press as: B.W. Xiong, Y.Y. Wang, Nuclear chiral doublet bands data tables, Atomic Data and Nuclear Data Tables (2018), https://doi.org/10.1016/j.adt.2018.05.002.

S. Muralithar, R. Kumar, R.P. Singh, M. Kumar Raju, Phys. Rev. C 92 (2015) 064307.
[91] E. Grodner, I. Sankowska, T. Morek, S.G. Rohoziński, Ch. Droste, J. Srebrny, A.A. Pasternak, M. Kisieliński, M. Kowalczyk, J. Kownacki, J. Mierzejewski, A. Król, K. Wrzosek, Phys. Lett. B 703 (2011) 46.
[92] E. Grodner, J. Srebrny, A.A. Pasternak, I. Zalewska, T. Morek, Ch. Droste, J. Mierzejewski, M. Kowalczyk, J. Kownacki, M. Kisieliński, S.G. Rohoziński, T. Koike, K. Starosta, A. Kordyasz, P.J. Napiorkowski, M. Wolińska-Cichocka, E. Ruchowska, W. Płóciennik, J. Perkowski, Phys. Rev. Lett. 97 (2006) 172501.
[93] A.J. Simons, P. Joshi, D.G. Jenkins, P.M. Raddon, R. Wadsworth, D.B. Fossan, T. Koike, C. Vaman, K. Starosta, E.S. Paul, H.J. Chantler, A.O. Evans, P. Bednarczyk, D. Curien, J. Phys. G: Nucl. Part. Phys. 31 (2005) 541.
[94] G. Rainovski, E.S. Paul, H.J. Chantler, P.J. Nolan, D.G. Jenkins, R. Wadsworth, P. Raddon, A. Simons, D.B. Fossan, T. Koike, K. Starosta, C. Vaman, E. Farnea, A. Gadea, Th. Kröll, R. Isocrate, G. de Angelis, D. Curien, V.I. Dimitrov, Phys. Rev. C 68 (2003) 024318.
[95] K.Y. Ma, J.B. Lu, D. Yang, H.D. Wang, Y.Z. Liu, X.G. Wu, Y. Zheng, C.Y. He, Phys. Rev. C 85 (2012) 037301.
[96] T. Koike, K. Starosta, C.J. Chiara, D.B. Fossan, D.R. LaFosse, Phys. Rev. C 63 (2001) 061304(R).
[97] I. Kuti, J. Timár, D. Sohler, E.S. Paul, K. Starosta, A. Astier, D. Bazzacco, P. Bednarczyk, A.J. Boston, N. Buforn, H.J. Chantler, C.J. Chiara, R.M. Clark, M. Cromaz, M. Descovich, Zs. Dombrádi, P. Fallon, D.B. Fossan, C. Fox, A. Gizon, J. Gizon, A.A. Hecht, N. Kintz, T. Koike, I.Y. Lee, S. Lunardi, A.O. Macchiavelli, P.J. Nolan, B.M. Nyakó, C.M. Petrache, J.A. Sampson, H.C. Scraggs, T.G. Tornyi, R. Wadsworth, A. Walker, L. Zolnai, Phys. Rev. C 87 (2013) 044323.
[98] C.M. Petrache, Q.B. Chen, S. Guo, A.D. Ayangeakaa, U. Garg, J.T. Matta, B.K. Nayak, D. Patel, J. Meng, M.P. Carpenter, C.J. Chiara, R.V.F. Janssens, F.G. Kondev, T. Lauritsen, D. Seweryniak, S. Zhu, S.S. Ghugre, R. Palit, Phys. Rev. C 94 (2016) 064309.
[99] R.A. Bark, A.M. Baxter, A.P. Byrne, G.D. Dracoulis, T. Kibédi, T.R. McGoram, S.M. Mullins, Nuclear Phys. A 691 (2001) 577.
[100] J. Timár, K. Starosta, I. Kuti, D. Sohler, D.B. Fossan, T. Koike, E.S. Paul, A.J. Boston, H.J. Chantler, M. Descovich, R.M. Clark, M. Cromaz, P. Fallon, I.Y. Lee, A.O. Macchiavelli, C.J. Chiara, R. Wadsworth, A.A. Hecht, D. Almehed, S. Frauendorf, Phys. Rev. C 84 (2011) 044302.
[101] C.M. Petrache, R. Venturelli, D. Vretenar, D. Bazzacco, G. Bonsignori, S. Brant, S. Lunardi, M.A. Rizzutto, C. Rossi Alvarez, G. de Angelis, M. De Poli, D.R. Napoli, Nuclear Phys. A 617 (1997) 228.
[102] D.J. Hartley, L.L. Riedinger, M.A. Riley, D.L. Balabanski, F.G. Kondev, R.W. Laird, J. Pfohl, D.E. Archer, T.B. Brown, R.M. Clark, M. Devlin, P. Fallon, I.M. Hibbert, D.T. Joss, D.R. LaFosse, P.J. Nolan, N.J. O'Brien, E.S. Paul, D.G. Sarantites, R.K. Sheline, S.L. Shepherd, J. Simpson, R. Wadsworth, Jing-ye Zhang, P.B. Semmes, F. Dönau, Phys. Rev. C 64 (2001) 031304(R).
[103] K.Y. Ma, J.B. Lu, Z. Zhang, J.Q. Liu, D. Yang, Y.M. Liu, X. Xu, X.Y. Li, Y.Z. Liu, X.G. Wu, Y. Zheng, C.B. Li, Phys. Rev. C 97 (2018) 014305.
[104] A.A. Hecht, C.W. Beausang, K.E. Zyromski, D.L. Balabanski, C.J. Barton, M.A. Caprio, R.F. Casten, J.R. Cooper, D.J. Hartley, R. Krücken, D. Meyer, H. Newman, J.R. Novak, E.S. Paul, N. Pietralla, A. Wolf, N.V. Zamfir, Jing-ye Zhang, F. Dönau, Phys. Rev. C 63 (2001) 051302(R).
[105] A.A. Hecht, C.W. Beausang, H. Amro, C.J. Barton, Z. Berant, M.A. Caprio, R.F. Casten, J.R. Cooper, D.J. Hartley, R. Krücken, D.A. Meyer, H. Newman, J.R. Novak, N. Pietralla, J.J. Ressler, A. Wolf, N.V. Zamfir, Jing-ye Zhang, K.E. Zyromski, Phys. Rev. C 68 (2003) 054310.
[106] D.L. Balabanski, M. Danchev, D.J. Hartley, L.L. Riedinger, O. Zeidan, Jing-ye Zhang, C.J. Barton, C.W. Beausang, M.A. Caprio, R.F. Casten, J.R. Cooper, A.A. Hecht, R. Krücken, J.R. Novak, N.V. Zamfir, K.E. Zyromski, Phys. Rev. C 70 (2004) 044305.
[107] J. Ndayishimye, E.A. Lawrie, O. Shirinda, J.L. Easton, S.M. Wyngaardt, R.A. Bark, S.P. Bvumbi, T.R.S. Dinoko, P. Jones, N.Y. Kheswa, J.J. Lawrie, S.N.T. Majola, P.L. Masiteng, D. Negi, J.N. Orce, P. Papka, J.F. Sharpey-Schafer, M. Stankiewicz, M. Wiedeking, Acta Phys. Polon. B 48 (2017) 343.
[108] P.L. Masiteng, E.A. Lawrie, T.M. Ramashidzha, J.J. Lawrie, R.A. Bark, R. Lindsay, F. Komati, J. Kau, P. Maine, S.M. Maliage, I. Matamba, S.M. Mullins, S.H.T. Murray, K.P. Mutshena, A.A. Pasternak, D.G. Roux, J.F. Sharpey-Schafer, O. Shirinda, P.A. Vymers, Eur. Phys. J. A 50 (2014) 119.
[109] E.A. Lawrie, P.A. Vymers, Ch. Vieu, J.J. Lawrie, C. Schück, R.A. Bark, R. Lindsay, G.K. Mabala, S.M. Maliage, P.L. Masiteng, S.M. Mullins, S.H.T. Murray, I. Ragnarsson, T.M. Ramashidzha, J.F. Sharpey-Schafer, O. Shirinda, Eur. Phys. J. A 45 (2010) 39.
[110] S.J. Zhu, J.H. Hamilton, A.V. Ramayya, P.M. Gore, J.O. Rasmussen, V. Dimitrov, S. Frauendorf, R.Q. Xu, J.K. Hwang, D. Fong, L.M. Yang, K. Li, Y.J. Chen, X.Q. Zhang, E.F. Jones, Y.X. Luo, I.Y. Lee, W.C. Ma, J.D. Cole, M.W. Drigert, M. Stoyer, G.M. Ter-Akopian, A.V. Daniel, Eur. Phys. J. A 25 (Suppl. 1) (2005) 459.
[111] Y.X. Luo, S.J. Zhu, J.H. Hamilton, J.O. Rasmussen, A.V. Ramayya, C. Goodin, K. Li, J.K. Hwang, D. Almehed, S. Frauendorf, V. Dimitrov, Jing-ye Zhang, X.L. Che, Z. Jang, I. Stefanescu, A. Gelberg, G.M. Ter-Akopian, A.V. Daniel, M.A. Stoyer, R. Donangelo, J.D. Cole, N.J. Stone, Phys. Lett. B 670 (2009) 307.
[112] S. Frauendorf, J. Meng, Z. Phys. A 356 (1996) 263.
[113] Y.H. Zhang, S.Q. Zhang, Q.Z. Zhao, S.F. Zhu, H.S. Xu, X.H. Zhou, Y.X. Guo, X.G. Lei, J. Lu, W.X. Huang, Q.B. Gou, H.J. Jin, Z. Liu, Y.X. Luo, X.F. Sun, Y.T. Zhu, X.G. Wu, S.X. Wen, C.X. Yang, Phys. Rev. C 60 (1999) 044311.
[114] C. Liu, Private Communication, January 2018.
[115] J.H. Hamilton, Y.X. Luo, S.J. Zhu, J.O. Rasmussen, A.V. Ramayya, C. Goodin, K. Li, J.K. Hwang, S. Liu, D. Almehed, S. Frauendorf, V. Dimitrov, Jing-ye Zhang, X.L. Che, Z. Jang, I. Stefanescu, A. Gelberg, G.M. Ter-Akopian, A.V. Daniel, I.Y. Lee, H.B. Ding, R.Q. Xu, J.G. Wang, Q. Xu, M.A. Stoyer, R. Donangelo, N.J. Stone, Acta Phys. Polon. B 40 (2009) 523.
[116] C. Vaman, (Ph.D. dissertation), State University of New York, 2004.
[117] J. Timár, C. Vaman, K. Starosta, D.B. Fossan, T. Koike, D. Sohler, I.Y. Lee, A.O. Macchiavelli, Phys. Rev. C 73 (2006) 011301(R).
[118] T. Suzuki, G. Rainovski, T. Koike, T. Ahn, M.P. Carpenter, A. Costin, M. Danchev, A. Dewald, R.V.F. Janssens, P. Joshi, C.J. Lister, O. Möller, N. Pietralla, T. Shinozuka, J. Timár, R. Wadsworth, C. Vaman, S. Zhu, Phys. Rev. C 78 (2008) 031302(R).
[119] J. Timár, Private Communication, December 2017.
[120] P. Joshi, S. Finnigan, D.B. Fossan, T. Koike, E.S. Paul, G. Rainovski, K. Starosta, C. Vaman, R. Wadsworth, J. Phys. G: Nucl. Part. Phys. 31 (2005) S1895.
[121] P. Joshi, M.P. Carpenter, D.B. Fossan, T. Koike, E.S. Paul, G. Rainovski, K. Starosta, C. Vaman, R. Wadsworth, Phys. Rev. Lett. 98 (2007) 102501.
[122] Y. Zheng, L.H. Zhu, X.G. Wu, C.Y. He, G.S. Li, X. Hao, B.B. Yu, S.H. Yao, B. Zhang, C. Xu, J.G. Wang, L. Gu, Chin. Phys. Lett. 31 (2014) 062101.
[123] N. Rather, P. Datta, S. Chattopadhyay, S. Rajbanshi, A. Goswami, G.H. Bhat, J.A. Sheikh, S. Roy, R. Palit, S. Pal, S. Saha, J. Sethi, S. Biswas, P. Singh, H.C. Jain, Phys. Rev. Lett. 112 (2014) 202503.
[124] R.A. Bark, E.O. Lieder, R.M. Lieder, E.A. Lawrie, J.J. Lawrie, S.P. Bvumbi, N.Y. Kheswa, S.S. Ntshangase, T.E. Madiba, P.L. Masiteng, S.M. Mullins, S. Murray, P. Papka, O. Shirinda, Q.B. Chen, S.Q. Zhang, Z.H. Zhang, P.W. Zhao, C. Xu, J. Meng, D.G. Roux, Z.P. Li, J. Peng, B. Qi, S.Y. Wang, Z.G. Xiao, Internat. J. Modern Phys. E 23 (2014) 1461001.
[125] B. Zhang, L.H. Zhu, H.B. Sun, C.Y. He, X.G. Wu, J.B. Lu, Y.J. Ma, X. Hao, Y. Zheng, B.B. Yu, G.S. Li, S.H. Yao, L.L. Wang, C. Xu, J.G. Wang, L. Gu, Chin. Phys. C 35 (2011) 1009.
[126] S.H. Yao, H.L. Ma, L.H. Zhu, X.G. Wu, C.Y. He, Y. Zheng, B. Zhang, G.S. Li, C.B. Li, S.P. Hu, X.P. Cao, B.B. Yu, C. Xu, Y.Y. Cheng, Phys. Rev. C 89 (2014) 014327.
[127] X.F. Li, Y.J. Ma, Y.Z. Liu, J.B. Lu, G.Y. Zhao, L.C. Yin, R. Meng, Z.L. Zhang, L.J. Wen, X.H. Zhou, Y.X. Guo, X.G. Lei, Z. Liu, J.J. He, Y. Zheng, Chin. Phys. Lett. 19 (2002) 1779.
[128] S.Y. Wang, Y.Z. Liu, T. Komatsubara, Y.J. Ma, Y.H. Zhang, Phys. Rev. C 74 (2006) 017302.
[129] K. Starosta, T. Koike, C.J. Chiara, D.B. Fossan, D.R. LaFosse, A.A. Hecht, C.W. Beausang, M.A. Caprio, J.R. Cooper, R. Krücken, J.R. Novak, N.V. Zamfir, K.E. Zyromski, D.J. Hartley, D.L. Balabanski, Jing-ye Zhang, S. Frauendorf, V.I. Dimitrov, Phys. Rev. Lett. 86 (2001) 971.
[130] L.L. Wang, X.G. Wu, L.H. Zhu, G.S. Li, X. Hao, Y. Zheng, C.Y. He, L. Wang, X.Q. Li, Y. Liu, B. Pan, Z.Y. Li, H.B. Ding, Chin. Phys. C 33 (2009) 173.
[131] X.G. Wu, L.L. Wang, L.H. Zhu, G.S. Li, X. Hao, Y. Zheng, C.Y. He, X.Q. Li, B. Pan, Y. Liu, L. Wang, Y.X. Zhao, Z.Y. Li, H.B. Ding, Plasma Sci. Technol. 14 (2012) 526.
[132] G. Rainovski, E.S. Paul, H.J. Chantler, P.J. Nolan, D.G. Jenkins, R. Wadsworth, P. Raddon, A. Simons, D.B. Fossan, T. Koike, K. Starosta, C. Vaman, E. Farnea, A. Gadea, Th. Kröll, G. de Angelis, R. Isocrate, D. Curien, V.I. Dimitrov, J. Phys. G: Nucl. Part. Phys. 29 (2003) 2763.
[133] C.M. Petrache, S. Brant, D. Bazzacco, G. Falconi, E. Farnea, S. Lunardi, V. Paar, Zs. Podolyák, R. Venturelli, D. Vretenar, Nuclear Phys. A 635 (1998) 361.
[134] C.M. Petrache, D. Bazzacco, S. Lunardi, C. Rossi Alvarez, G. de Angelis, M. De Poli, D. Bucurescu, C.A. Ur, P.B. Semmes, R. Wyss, Nuclear Phys. A 597 (1996) 106.
[135] C.M. Petrache, G.B. Hagemann, I. Hamamoto, K. Starosta, Phys. Rev. Lett. 96 (2006) 112502.
[136] D. Tonev, P. Petkov, D.L. Balabanski, G. de Angelis, A. Gadea, D.R. Napoli, N. Marginean, A. Dewald, P. Pejovic, A. Fitzler, O. Möller, K.O. Zell, S. Brant, S. Frauendorf, D. Bazzacco, S. Lenzi, S. Lunardi, P. Bednarczyk, D. Curien, C. Petrache, Q. Zhong, Y.H. Zhang, Jing-ye Zhang, Internat. J. Modern Phys. E 15 (2006) 1531.
[137] D. Tonev, G. de Angelis, S. Brant, S. Frauendorf, P. Petkov, A. Dewald, F. Dönau, D.L. Balabanski, Q. Zhong, P. Pejovic, D. Bazzacco, P. Bednarczyk, F. Camera, D. Curien, F. Della Vedova, A. Fitzler, A. Gadea, G. Lo Bianco, S. Lenzi, S. Lunardi, N. Marginean, O. Möller, D.R. Napoli, R. Orlandi, E. Sahin, A. Saltarelli, J. Valiente Dobon, K.O. Zell, Jing-ye Zhang, Y.H. Zhang, Phys. Rev. C 76 (2007) 044313.
[138] S. Zhu, U. Garg, B.K. Nayak, S.S. Ghugre, N.S. Pattabiraman, D.B. Fossan, T. Koike, K. Starosta, C. Vaman, R.V.F. Janssens, R.S. Chakrawarthy, M.

Please cite this article in press as: B.W. Xiong, Y.Y. Wang, Nuclear chiral doublet bands data tables, Atomic Data and Nuclear Data Tables (2018), https://doi.org/10.1016/j.adt.2018.05.002.

Whitehead, A.O. Macchiavelli, S. Frauendorf, Phys. Rev. Lett. 91 (2003) 132501.

[139] E. Mergel, C.M. Petrache, G. Lo Bianco, H. Hübel, J. Domscheit, D. Roßbach, G. Schönwaßer, N. Nenoff, A. Neußer, A. Görgen, F. Becker, E. Bouchez, M. Houry, A. Hürstel, Y.L. Coz, R. Lucas, Ch. Theisen, W. Korten, A. Bracco, N. Blasi, F. Camera, S. Leoni, F. Hannachi, A. Lopez-Martens, M. Rejmund, D. Gassmann, P. Reiter, P.G. Thirolf, A. Astier, N. Buforn, M. Meyer, N. Redon, O. Stezowski, Eur. Phys. J. A 15 (2002) 417.

[140] S. Mukhopadhyay, D. Almehed, U. Garg, S. Frauendorf, T. Li, P.V. Madhusudhana Rao, X. Wang, S.S. Ghugre, M.P. Carpenter, S. Gros, A. Hecht, R.V.F. Janssens, F.G. Kondev, T. Lauritsen, D. Seweryniak, S. Zhu, Phys. Rev. C 78 (2008) 034311.

[141] C.W. Beausang, A.A. Hecht, K.E. Zyromski, D. Balabanski, C.J. Barton, M.A. Caprio, R.F. Casten, J.R. Cooper, D. Hartley, R. Krücken, J.R. Novak, N.V. Zamfir, Jing-ye Zhang, F. Dönau, Nuclear Phys. A 682 (2001) 394c.

[142] A.A. Hecht, (Ph.D. dissertation), Yale University, 2004.

[143] P.L. Masiteng, E.A. Lawrie, T.M. Ramashidzha, R.A. Bark, B.G. Carlsson, J.J. Lawrie, R. Lindsay, F. Komati, J. Kau, P. Maine, S.M. Maliage, I. Matamba, S.M. Mullins, S.H.T. Murray, K.P. Mutshena, A.A. Pasternak, I. Ragnarsson, D.G. Roux, J.F. Sharpey-Schafer, O. Shirinda, P.A. Vymers, Phys. Lett. B 719 (2013) 83.

[144] P.L. Masiteng, A.A. Pasternak, E.A. Lawrie, O. Shirinda, J.J. Lawrie, R.A. Bark, S.P. Bvumbi, N.Y. Kheswa, R. Lindsay, E.O. Lieder, R.M. Lieder, T.E. Madiba, S.M. Mullins, S.H.T. Murray, J. Ndayishimye, S.S. Ntshangase, P. Papka, J.F. Sharpey-Schafer, Eur. Phys. J. A 52 (2016) 28.

[145] E.A. Lawrie, P.A. Vymers, J.J. Lawrie, Ch. Vieu, R.A. Bark, R. Lindsay, G.K. Mabala, S.M. Maliage, P.L. Masiteng, S.M. Mullins, S.H.T. Murray, I. Ragnarsson, T.M. Ramashidzha, C. Schück, J.F. Sharpey-Schafer, O. Shirinda, Phys. Rev. C 78 (2008) 021305(R).

Please cite this article in press as: B.W. Xiong, Y.Y. Wang, Nuclear chiral doublet bands data tables, Atomic Data and Nuclear Data Tables (2018), https://doi.org/10.1016/j.adt.2018.05.002.

Explanation of Tables

Table 1. **Chiral doublet bands.**

${}^{A}_{Z}X_{N}$	Denotes the specific nuclide with X chemical symbol A mass number Z atomic number N neutron number A horizontal line connecting a row marks the end of entry for each chiral nucleus. For multiple chiral doublet bands, the pairs of chiral doublet bands are separated by a horizontal line starting from the second column.
I^{π}	I denotes the level spin in units of $\hbar$ for each band member. π denotes the parity (+or −). References for each nucleus are given directly in last column.
E	Level energy in units of keV. The number of digits follows the original experimental article. In the energy column, yrast and side denote the two partners of chiral doublet bands. The star marks the level which is the yrast state (the lowest state for given spin) in the nucleus.
$B(M1)/B(E2)$	The ratio of reduced transition strength in units of $\mu_N^2/\mathrm{e}^2\mathrm{b}^2$ with the uncertainties available in parentheses. The number of digits follow the original experimental article. In the $B(M1)/B(E2)$ column, yrast and side denote the two partners of chiral doublet bands. For the nuclei ^{106}Mo, ^{98}Tc, ^{100}Tc, ^{110}Ru, ^{112}Ru, ^{102}Rh, ^{106}Rh, ^{111}Rh, ^{113}Rh, ^{104}Ag, ^{126}I, ^{128}Cs, ^{132}Cs, ^{132}La, ^{134}La, ^{134}Pr, ^{136}Nd, ^{137}Nd, ^{138}Nd, ^{188}Ir, and ^{198}Tl, the $B(M1)/B(E2)$ ratios are extracted by the equation (2) in Ref. [113]. For the nuclei ^{104}Rh, ^{106}Ag, ^{107}Ag, ^{124}Cs, ^{126}Cs, ^{130}Cs, ^{135}Nd, and ^{194}Tl with $B(M1)$ and $B(E2)$ values available, the $B(M1)/B(E2)$ ratios are also calculated. For experimental data available, the number of digits follows the significant digits of the error. For the data which extracted from the experimental article, the number of digits is determined by the original data according to the error transfer formula.

Table 2. **Chiral doublet bands with $B(M1)$ and $B(E2)$ values.**

${}^{A}_{Z}X_{N}$	Same as the explanation in Table 1.
I^{π}	Same as the explanation in Table 1.
E	Same as the explanation in Table 1.
$B(M1)$	The magnetic dipole transition strength in units of μ_N^2 with the uncertainties available in parentheses. The number of digits follows the original experimental article. In the $B(M1)$ column, yrast and side denote the two partners of chiral doublet bands.
$B(E2)$	The electric quadrupole transition strength in units of $\mathrm{e}^2\mathrm{b}^2$ with the uncertainties available in parentheses. The number of digits follows the original experimental article. In the $B(E2)$ column, yrast and side denote the two partners of chiral doublet bands.

Please cite this article in press as: B.W. Xiong, Y.Y. Wang, Nuclear chiral doublet bands data tables, Atomic Data and Nuclear Data Tables (2018), https://doi.org/10.1016/j.adt.2018.05.002.

Table 1
Chiral doublet bands. See Explanation of Tables for details.

Nuclei	$I^{\pi}(\hbar)$	E (keV)		$B(M1)/B(E2)$ (μ_N^2/e^2b^2)		References
		yrast	side	yrast	side	
$^{78}_{35}Br_{43}$	8^+	465.7*				[55,114]
	9^+	975.3*	1408.6			
	10^+	1369.4*	1881.5	2.13918 $(^{+0.07423}_{-0.07423})$		
	11^+	1937.8*	2482.8	10.56231 $(^{+0.92806}_{-0.92806})$	6.15398 $(^{+0.88693}_{-0.88693})$	
	12^+	2582.5*	2975.9	< 0.82258	1.6983 $(^{+0.40338}_{-0.40338})$	
	13^+	3146.0*	3644.4	7.4299 $(^{+0.6144}_{-0.6144})$		
	14^+	4046.2*		< 1.85685		
	15^+	4539.0*		8.02873 $(^{+1.56134}_{-1.56134})$		
	16^+	5600.2*				
	17^+	6084.6*				
	18^+	7268.2				
	19^+	7818.4				
	20^+	9132.2				
	6^-	422.6	601.1			[55,114]
	7^-	683.4	828.6			
	8^-	1028.5	1190.2	0.31614 $(^{+0.07277}_{-0.07277})$	0.17 $(^{+0.08}_{-0.08})$	
	9^-	1461.1	1602.8	1.30596 $(^{+0.29978}_{-0.29978})$	0.65 $(^{+0.13}_{-0.13})$	
	10^-	1902.8	2026.3	< 0.39233	< 0.2717	
	11^-	2452.8	2666.5	2.53562 $(^{+1.14277}_{-1.14277})$	< 0.64594	
	12^-	3013.8	3073.1	< 1.12632	< 1.3865	
	13^-	3616.8		4.08762 $(^{+1.65843}_{-1.65843})$		
	14^-	4292.0	4319.4			
	15^-	4919.5				
	16^-	5764.0				
	17^-	6412.3				
	19^-	8045.1				
$^{80}_{35}Br_{45}$	6^+	357.1*				[74]
	7^+	447.7*				
	8^+	616.0*				
	9^+	1141.6*	1534.8	7.6744 $(^{+1.6049}_{-1.6049})$		
	10^+	1588.7*	2002.2	1.5662 $(^{+0.1989}_{-0.1989})$		
	11^+	2257.6*	2681.4	17.8417 $(^{+3.3394}_{-3.3394})$	7.3 $(^{+1.8}_{-1.8})$	
	12^+	2945.4*	3212.9	1.9518 $(^{+0.2036}_{-0.2036})$	5.3 $(^{+1.3}_{-1.3})$	
	13^+	3658.7*	3972.9	6.206 $(^{+1.8574}_{-1.8574})$		
	14^+	4451.8*		0.2253 $(^{+0.0484}_{-0.0484})$		
	15^+	5195.2				
	16^+	5936.5				
$^{106}_{42}Mo_{64}$	4^-		1937.0			[75,110]
	5^-	1952.4	2090.6			
	6^-	2142.9	2276.5			
	7^-	2369.5	2499.0	0.58	0.22	
	8^-	2630.1	2746.6	0.40	0.16	
	9^-	2922.3	3041.7	0.25	0.15	
	10^-	3239.5	3349.8	0.22	0.28	
	11^-	3592.8	3707.7	< 0.55	0.42	
	12^-	3946.4	4049.4	< 0.58	< 0.49	
	13^-	4372.7				
	14^-	4753.2				
$^{98}_{43}Tc_{55}$	9^-	1166.2				[76]
	10^-	1582.5	1920.6	9.7		
	11^-	1851.4*	2368.8	7.2		
	12^-	2303.9*	2671.1	5.9	3.0	
	13^-	2677.4*	3266.3	2.4	< 1.9	
	14^-	3130.2*		1.9		
	15^-	3724.7		0.9		
$^{100}_{43}Tc_{57}$	9^-	778*				[77]
	10^-	1155*	1583			

(*continued on next page*)

Please cite this article in press as: B.W. Xiong, Y.Y. Wang, Nuclear chiral doublet bands data tables, Atomic Data and Nuclear Data Tables (2018), https://doi.org/10.1016/j.adt.2018.05.002.

Table 1 (*continued*)

Nuclei	$I^{\pi}(\hbar)$	E (keV)		$B(M1)/B(E2)$ (μ_N^2/e^2b^2)		References
		yrast	side	yrast	side	
	11^-	1406*	2055	6.55 $(^{+0.04}_{-0.04})$		
	12^-	1840*	2394	10.34 $(^{+0.17}_{-0.17})$	12.93 $(^{+4.14}_{-4.14})$	
	13^-	2238*	2802	2.67 $(^{+0.02}_{-0.02})$		
	14^-	2693*	3273	6.41 $(^{+0.46}_{-0.46})$		
	15^-	3234*	3693	1.71 $(^{+0.18}_{-0.18})$		
	16^-	3713*		2.99 $(^{+0.32}_{-0.32})$		
	17^-	4357*		3.13 $(^{+1.74}_{-1.74})$		
$^{110}_{44}Ru_{66}$	4^-		2016.2			[75,78,111,115]
	5^-		2145.3			
	6^-	2242.9	2328.0			
	7^-	2426.5	2516.7			
	8^-	2637.4	2764.7	0.38	0.30	
	9^-	2892.7	3041.4	0.40	0.24	
	10^-	3175.3	3337.1	0.29	0.48	
	11^-	3485.3*	3689.9	0.42	0.23	
	12^-	3818.5	4038.8	0.32	0.63	
	13^-	4195.5*	4446.3	< 0.77		
	14^-	4566.5	4874.1			
	15^-	5010.8*	5302.5			
	16^-	5412.8				
$^{112}_{44}Ru_{68}$	5^-	2003.2				[75,78,111,115]
	6^-	2230.2	2334.2			
	7^-	2489.2	2574.3			
	8^-	2771.7	2829.2	0.50		
	9^-	3076.5	3094.1	0.29	0.20	
	10^-	3420.8	3379.8	0.40	0.38	
	11^-	3768.3	3711.5	0.67	0.34	
	12^-	4198.8	4032.5	0.71	< 0.91	
	13^-	4561.7	4428.3			
	14^-	5072.9	4769.6			
	15^-		5227.8			
$^{102}_{45}Rh_{57}$	8^-	78				[79,116]
	9^-	224				
	10^-	587*	1048	6.32 $(^{+0.53}_{-0.53})$		
	11^-	893*	1500	11.42 $(^{+0.79}_{-0.79})$		
	12^-	1355*	1859	11.27 $(^{+0.83}_{-0.83})$	4.24 $(^{+0.63}_{-0.63})$	
	13^-	1793*	2323	7.37 $(^{+0.50}_{-0.50})$	6.94 $(^{+2.44}_{-2.44})$	
	14^-	2281*		15.61 $(^{+1.37}_{-1.37})$	22.82 $(^{+5.48}_{-5.48})$	
	15^-	2809*		7.16 $(^{+0.70}_{-0.70})$		
	16^-	3337*		10.85 $(^{+1.18}_{-1.18})$		
	17^-	3939*		7.87 $(^{+0.79}_{-0.79})$		
	18^-	4544*		10.49 $(^{+1.50}_{-1.50})$		
$^{103}_{45}Rh_{58}$	10.5^+	3238				[54,117–119]
	11.5^+	3357				
	12.5^+	3591		23.9 $(^{+8.3}_{-8.3})$		
	13.5^+	3899	4445	14.2 $(^{+1.8}_{-1.8})$		
	14.5^+	4281	4789	11.4 $(^{+1.6}_{-1.6})$		
	15.5^+	4665	5166	12.2 $(^{+2.1}_{-2.1})$	12.1 $(^{+2.9}_{-2.9})$	
	16.5^+	5156	5616	13.3 $(^{+1.7}_{-1.7})$	10.3 $(^{+3.0}_{-3.0})$	
	17.5^+	5622	6062	11.8 $(^{+1.7}_{-1.7})$	5.7 $(^{+1.3}_{-1.3})$	
	18.5^+	6163	6528	15.1 $(^{+3.2}_{-3.2})$	23.9 $(^{+12.7}_{-12.7})$	
	19.5^+	6706	7074	15.0 $(^{+5.2}_{-5.2})$	9.0 $(^{+5.0}_{-5.0})$	
	20.5^+	7317		22.8 $(^{+9.8}_{-9.8})$		
	21.5^+	7952		17.4 $(^{+8.5}_{-8.5})$		
	6.5^-	2033				[54,117–119]
	7.5^-	2219				
	8.5^-	2343		40.6 $(^{+7.3}_{-7.3})$		

(*continued on next page*)

Please cite this article in press as: B.W. Xiong, Y.Y. Wang, Nuclear chiral doublet bands data tables, Atomic Data and Nuclear Data Tables (2018), https://doi.org/10.1016/j.adt.2018.05.002.

Table 1 (*continued*)

Nuclei	$I^{\pi}(\hbar)$	E (keV)		$B(M1)/B(E2)$ (μ_N^2/e^2b^2)		References
		yrast	side	yrast	side	
	9.5^-	2538	2744	$25.0\,(^{+3.3}_{-3.3})$		
	10.5^-	2751	2934	$37.1\,(^{+5.8}_{-5.8})$		
	11.5^-	3011*	3273	$16.8\,(^{+2.0}_{-2.0})$		
	12.5^-	3327*	3615	$16.8\,(^{+3.6}_{-3.6})$	$21.1\,(^{+2.5}_{-2.5})$	
	13.5^-	3769*	4080	$12.9\,(^{+2.2}_{-2.2})$	$12.6\,(^{+1.5}_{-1.5})$	
	14.5^-	4195	4559	$10.0\,(^{+2.4}_{-2.4})$	$10.2\,(^{+1.5}_{-1.5})$	
	15.5^-	4763	5091	$13.4\,(^{+3.0}_{-3.0})$	$5.4\,(^{+1.5}_{-1.5})$	
	16.5^-	5297	5685	$6.7\,(^{+1.0}_{-1.0})$	$6.8\,(^{-3.9}_{-3.9})$	
	17.5^-	5923		$11.3\,(^{+2.9}_{-2.9})$		
	18.5^-	6586		$4.3\,(^{+1.5}_{-1.5})$		
	19.5^-	7186		$12.4\,(^{+5.4}_{-5.4})$		
	6.5^-	2228				[54,117–119]
	7.5^-	2366	2443			
	8.5^-	2520	2643			
	9.5^-	2699	2871	$30.8\,(^{+4.8}_{-4.8})$	$10.3\,(^{+3.5}_{-3.5})$	
	10.5^-	2915	3090	$18.2\,(^{+2.0}_{-2.0})$	$33.1\,(^{+13.4}_{-13.4})$	
	11.5^-	3227	3416	$28.2\,(^{+9.7}_{-9.7})$	$15.2\,(^{+5.1}_{-5.1})$	
	12.5^-	3668	3778	$17.7\,(^{+2.5}_{-2.5})$	$13.7\,(^{+3.0}_{-3.0})$	
	13.5^-	4106	4210	$3.8\,(^{+0.5}_{-0.5})$	$10.2\,(^{+2.6}_{-2.6})$	
	14.5^-	4606	4659	$5.3\,(^{+0.5}_{-0.5})$	$11.9\,(^{+3.4}_{-3.4})$	
	15.5^-	5061	5059	$2.7\,(^{+0.6}_{-0.6})$		
	16.5^-	5577		$4.3\,(^{+1.0}_{-1.0})$		
	17.5^-	6143		$6.8\,(^{+3.5}_{-3.5})$		
$^{104}_{45}Rh_{59}$	9^-	483*				[80,118]
	10^-	840*	1228	$15.079\,(^{+2.643}_{-2.643})$		
	11^-	1168*	1582	$9.785\,(^{+1.483}_{-1.483})$		
	12^-	1636*	1971	$11.282\,(^{+1.384}_{-1.384})$		
	13^-	2111*	2370	$6.289\,(^{+0.646}_{-0.646})$		
	14^-	2639*	2834			
	15^-	3229*	3320			
	16^-	3800*	3876			
	17^-	4406	4406			
$^{105}_{45}Rh_{60}$	11.5^+	2982*				[57,58,119]
	12.5^+	3198*				
	13.5^+	3478*	4003	$9.9\,(^{+1.8}_{-1.8})$		
	14.5^+	3839*	4299	$15.6\,(^{+3.6}_{-3.6})$		
	15.5^+	4215*	4690	$13.6\,(^{+3.2}_{-3.2})$	$8.2\,(^{+2.7}_{-2.7})$	
	16.5^+	4702*	5081	$14.4\,(^{+2.9}_{-2.9})$	$11.1\,(^{+3.2}_{-3.2})$	
	17.5^+	5184	5525	$13.5\,(^{+2.8}_{-2.8})$	$8.6\,(^{+2.5}_{-2.5})$	
	18.5^+	5764	6020	$13.4\,(^{+2.9}_{-2.9})$	$9.1\,(^{+2.7}_{-2.7})$	
	19.5^+	6345	6566	$11.3\,(^{+2.2}_{-2.2})$	$7.5\,(^{+2.6}_{-2.6})$	
	20.5^+	7038	7156	$10.8\,(^{+2.9}_{-2.9})$	$8.2\,(^{+4.4}_{-4.4})$	
	21.5^+	7713		$8.4\,(^{+3.0}_{-3.0})$		
	22.5^+	8467	8524	$9.6\,(^{+5.4}_{-5.4})$		
	23.5^+	9213				
	7.5^-		2417			[57]
	8.5^-	2478	2512			
	9.5^-	2670	2645			
	10.5^-	2915	2824			
	11.5^-	3268	3077			
	12.5^-	3669	3469			
	13.5^-	4094				
$^{106}_{45}Rh_{61}$	9^-	428*				[81]
	10^-	761*	1053	$8.87\,(^{+2.42}_{-2.42})$		

(*continued on next page*)

Please cite this article in press as: B.W. Xiong, Y.Y. Wang, Nuclear chiral doublet bands data tables, Atomic Data and Nuclear Data Tables (2018), https://doi.org/10.1016/j.adt.2018.05.002.

Table 1 (*continued*)

Nuclei	$I^{\pi}(\hbar)$	E (keV)		$B(M1)/B(E2)$ (μ_N^2/e^2b^2)		References
		yrast	side	yrast	side	
	11^-	1071*	1410	$5.66\,(^{+0.30}_{-0.30})$		
	12^-	1488*	1787	$8.13\,(^{+0.92}_{-0.92})$	$59.10\,(^{+61.39}_{-61.39})$	
	13^-	1905*	2258	$4.66\,(^{+0.36}_{-0.36})$	$2.23\,(^{+0.82}_{-0.82})$	
	14^-	2359*	2730	$6.92\,(^{+0.58}_{-0.58})$	$10.11\,(^{+6.10}_{-6.10})$	
	15^-	2859*	3214	$4.52\,(^{+0.45}_{-0.45})$	$5.68\,(^{+2.94}_{-2.94})$	
	16^-	3323*	3708	$5.93\,(^{+0.60}_{-0.60})$	$6.06\,(^{+9.90}_{-9.90})$	
	17^-	3864*		$4.44\,(^{+0.91}_{-0.91})$		
	18^-	4320*		$7.27\,(^{+1.87}_{-1.87})$		
	19^-	4861*		$3.77\,(^{+1.59}_{-1.59})$		
	20^-	5363*		$3.85\,(^{+1.01}_{-1.01})$		
	21^-	5948*		$4.57\,(^{+2.28}_{-2.28})$		
	22^-	6533*		$4.64\,(^{+2.59}_{-2.59})$		
$^{111}_{45}Rh_{66}$	10.5^+	2112.7*				[82]
	11.5^+	2355.4*	2733.2		2.39	
	12.5^+	2650.8*	2984.5	4.79	8.25	
	13.5^+	2964.4*	3272.3	5.74		
	14.5^+	3325.4*	3523.9	4.92	4.09	
	15.5^+	3742.5*	3933.4			
	16.5^+		4249.3*			
$^{113}_{45}Rh_{68}$	9.5^+	1775.5*		3.27		[82]
	10.5^+	2038.0*	2133.2	3.23		
	11.5^+	2470.3	2446.5*	1.90		
	12.5^+	2723.3*	2776.9	4.47	3.84	
	13.5^+	3090.9*	3133.0	3.23		
	14.5^+	3334.8*				
	15.5^+	3770.2*				
	16.5^+	4006.0*				
$^{104}_{47}Ag_{57}$	8^-	1077				[83]
	9^-	1253				
	10^-	1599*	2212			
	11^-	1932*	2711	$13.3\,(^{+1.8}_{-1.8})$		
	12^-	2376*	3040	$11.9\,(^{+2.7}_{-2.7})$	$13.0\,(^{+5.0}_{-5.0})$	
	13^-	2820*	3351	$12.2\,(^{+3.2}_{-3.2})$	$18.4\,(^{+8.3}_{-8.3})$	
	14^-	3301*	3648	$14.1\,(^{+3.8}_{-3.8})$		
	15^-	3809*	4097	$14.4\,(^{+3.2}_{-3.2})$		
	16^-	4329*	4625	$14.1\,(^{+2.2}_{-2.2})$	$17.2\,(^{+6.8}_{-6.8})$	
	17^-	4901*		$11.7\,(^{+3.0}_{-3.0})$		
	18^-	5529*		$16.3\,(^{+5.7}_{-5.7})$		
	19^-	6133				
$^{105}_{47}Ag_{58}$	7.5^-		2622.2			[84]
	8.5^-		2775.2			
	9.5^-	2908.2	2944.2			
	10.5^-	3102.2	3177.2			
	11.5^-	3409.2	3481.2			
	12.5^-	3786.2	3867.2		$17.0\,(^{+4.4}_{-4.4})$	
	13.5^-	4250.2	4314.2	$8.0\,(^{+1.6}_{-1.6})$	$10.7\,(^{+1.9}_{-1.9})$	
	14.5^-	4719.2	4797.2	$14.2\,(^{+3.1}_{-3.1})$	$12.1\,(^{+2.5}_{-2.5})$	
	15.5^-	5227.2	5335.2	$6.5\,(^{+2.0}_{-2.0})$	$8.2\,(^{+4.3}_{-4.3})$	
$^{106}_{47}Ag_{59}$	10^-	2271.7	3203.8			[85,120–124]
	11^-	2441.4	3423.5			
	12^-	2660.4	3676.0			
	13^-	2930.2	3941.6			

(*continued on next page*)

Please cite this article in press as: B.W. Xiong, Y.Y. Wang, Nuclear chiral doublet bands data tables, Atomic Data and Nuclear Data Tables (2018), https://doi.org/10.1016/j.adt.2018.05.002.

Table 1 (*continued*)

Nuclei	$I^{\pi}(\hbar)$	E (keV)		$B(M1)/B(E2)$ (μ_N^2/e^2b^2)		References
		yrast	side	yrast	side	
	14^-	3256.7	4263.7	$13.350\,(^{+6.980}_{-6.980})$		
	15^-	3686.1	4636.6	$9.132\,(^{+2.633}_{-2.633})$	$11.675\,(^{+4.845}_{-4.845})$	
	16^-	4223.3*	5051.7	$5.444\,(^{+1.273}_{-1.273})$	$8.797\,(^{+2.337}_{-2.337})$	
	17^-	4742.6*	5561.2	$4.584\,(^{+1.313}_{-1.313})$	$6.863\,(^{+2.269}_{-2.269})$	
	18^-	5414.9*	6065.8	$7.471\,(^{+4.078}_{-4.078})$	$6.391\,(^{+2.115}_{-2.115})$	
	19^-	6026.8*	6691.0	$5.686\,(^{+1.459}_{-1.459})$	$5.434\,(^{+2.013}_{-2.013})$	
	20^-	6760.7*	7276.7	$6.721\,(^{+2.400}_{-2.400})$	$6.544\,(^{+3.018}_{-3.018})$	
	21^-	7531.7	7945.6	$1.857\,(^{+1.092}_{-1.092})$		
	22^-	8192.5				
$^{107}_{47}Ag_{60}$	10.5^-	2620.8*	2901.6			[60,125,126]
	11.5^-	2928.7*	3091.8	$6.94\,(^{+3.06}_{-3.06})$		
	12.5^-	3338.7*	3392.0	$9.11\,(^{+2.85}_{-2.85})$		
	13.5^-	3800.0	3897.5	$10.63\,(^{+3.40}_{-3.40})$		
	14.5^-	4270.0	4349.6	6.50		
	15.5^-	4878.8	4932.0			
	16.5^-	5437.3				
	11.5^+	3334.8				[60,61,125,126]
	12.5^+	3556.7		$34.67\,(^{+22.29}_{-22.29})$		
	13.5^+	3851.3		$11.74\,(^{+3.65}_{-3.65})$		
	14.5^+	4230.0*	4841.7	$12.00\,(^{+3.12}_{-3.12})$		
	15.5^+	4626.4*	5131.1	$13.57\,(^{+3.61}_{-3.61})$		
	16.5^+	5120.5*	5448.9	$8.26\,(^{+2.77}_{-2.77})$		
	17.5^+	5621.5*	5818.4	7.81		
	18.5^+	6192.8*	6250.2			
	19.5^+	6785.9	6761.3*			
	20.5^+	7441.1	7315.5*			
	21.5^+		7919.9*			
	22.5^+		8591.2*			
$^{118}_{53}I_{65}$	7^-	0*				[86]
	8^-	123*				
	9^-	353*	821			
	10^-	647*	1025			
	11^-	980*	1332			
	12^-	1343*	1702			
	13^-	1733*	2111			
	14^-	2149*	2550			
	15^-	2588				
$^{123}_{53}I_{70}$	10.5^+		2876			[87]
	11.5^+	3083	3200	$1.0\,(^{+0.3}_{-0.3})$	$2.55\,(^{+0.45}_{-0.45})$	
	12.5^+	3324*	3490	$1.1\,(^{+0.4}_{-0.4})$	$1.75\,(^{+0.35}_{-0.35})$	
	13.5^+	3716	3903	$0.9\,(^{+0.5}_{-0.5})$	$1.80\,(^{+0.50}_{-0.50})$	
	14.5^+	4055*	4250		$1.53\,(^{+0.60}_{-0.60})$	
	15.5^+	4542	4699			
	16.5^+	4901*				
	18.5^+	5819*				
	20.5^+	6863*				
$^{126}_{53}I_{73}$	8^-	410.7*				[88]
	9^-	735.1*				

(*continued on next page*)

Please cite this article in press as: B.W. Xiong, Y.Y. Wang, Nuclear chiral doublet bands data tables, Atomic Data and Nuclear Data Tables (2018), https://doi.org/10.1016/j.adt.2018.05.002.

Table 1 (*continued*)

Nuclei	$I^{\pi}(\hbar)$	E (keV)		$B(M1)/B(E2)$ (μ_N^2/e^2b^2)		References
		yrast	side	yrast	side	
	10^-	1129.7*		$1.44\,(^{+0.03}_{-0.03})$		
	11^-	1468.4*	2213.7	$1.83\,(^{+0.04}_{-0.04})$		
	12^-	1893.7*	2432.7	$1.53\,(^{+0.05}_{-0.05})$		
	13^-	2322.1*	2707.6	$0.22\,(^{+0.01}_{-0.01})$	$3.73\,(^{+0.15}_{-0.15})$	
	14^-	2759.1*	2959.4	$3.02\,(^{+0.16}_{-0.16})$	$5.49\,(^{+0.46}_{-0.46})$	
	15^-	3290.4	3358.6	$0.32\,(^{+0.03}_{-0.03})$	$9.47\,(^{+0.86}_{-0.86})$	
	16^-	3674.5	3745.9	$4.95\,(^{+0.42}_{-0.42})$	$4.00\,(^{+0.50}_{-0.50})$	
	17^-	4184.1	4235.6	$< 1.84\,(^{+0.09}_{-0.09})$	$3.00\,(^{+0.38}_{-0.38})$	
	18^-	4534.1	4649.9	$1.39\,(^{+0.14}_{-0.14})$		
	19^-	5143.0		$< 5.56\,(^{+0.62}_{-0.62})$		
	20^-	5528.9		$\sim 1.48\,(^{+0.18}_{-0.18})$		
	21^-	6231.5		$\sim 0.44\,(^{+0.06}_{-0.06})$		
	22^-	6659.7				
$^{122}_{55}Cs_{67}$	10^+	368.4*				[89]
	11^+	674.4*	915.4			
	12^+	840.8*	1221.5			
	13^+	1233.2*	1492.2			
	14^+	1499.9*	1911.7			
	15^+	1937.3*	2227.3			
	16^+	2313.8*	2757.2			
	17^+	2769.1*	3093.2			
	18^+	3250.8*				
	19^+	3706.8*	4048.0			
	20^+	4284.7*				
	21^+	4731.5*				
$^{124}_{55}Cs_{69}$	8^+	561.9*				[90]
	9^+	619.9*				
	10^+	743.9*				
	11^+	1055.9*	1260.2			
	12^+	1275.9*	1631.2			
	13^+	1673.9*	1893.2			
	14^+	1989.9*	2265.2	$0.86\,(^{+0.24}_{-0.31})$	$1.37\,(^{+0.60}_{-0.63})$	
	15^+	2446.9*	2666.2	$3.40\,(^{+1.11}_{-1.53})$	$2.69\,(^{+0.98}_{-0.87})$	
	16^+	2858.9*	3090.2	$0.22\,(^{+0.06}_{-0.05})$	$0.42\,(^{+0.16}_{-0.16})$	
	17^+	3344.9*	3574.2	$2.95\,(^{+1.15}_{-0.75})$	$1.62\,(^{+0.73}_{-0.60})$	
	18^+	3832.9*		$0.28\,(^{+0.06}_{-0.06})$		
	19^+	4342.9*		$3.02\,(^{+0.68}_{-0.82})$		
	20^+	4906.9*		$0.28\,(^{+0.07}_{-0.07})$		
	21^+	5424.9*		$2.44\,(^{+1.19}_{-1.14})$		
	22^+	6086.9*		$0.32\,(^{+0.06}_{-0.06})$		
	23^+	6550.9		$2.44\,(^{+0.68}_{-0.68})$		
	24^+	7357.9				
	25^+	7649.9				
$^{126}_{55}Cs_{71}$	9^+	0*				[91,127,128]
	10^+	140*				
	11^+	477*	637			
	12^+	732*	999			
	13^+	1128*	1326			
	14^+	1471*	1671	$0.64\,(^{+0.44}_{-0.12})$	$1.26\,(^{+0.64}_{-0.26})$	
	15^+	1935*	2097	$4.43\,(^{+3.71}_{-1.04})$	$3.04\,(^{+2.75}_{-0.85})$	
	16^+	2350*	2572	$0.26\,(^{+0.10}_{-0.04})$	$1.47\,(^{+0.90}_{-0.23})$	
	17^+	2846*	3033	$2.95\,(^{+1.96}_{-0.62})$	$0.92\,(^{+0.58}_{-0.19})$	
	18^+	3311*		$0.48\,(^{+0.16}_{-0.07})$		
	19^+	3839*	4040	$3.63\,(^{+3.50}_{-1.05})$		
	20^+	4357*		$0.83\,(^{+0.40}_{-0.11})$		
	21^+	4911*		$2.65\,(^{+3.75}_{-1.21})$		
$^{128}_{55}Cs_{73}$	9^+	0*				[24,92,96]
	10^+	143*				
	11^+	492*	652			
	12^+	765*	1024	2.2		

(*continued on next page*)

Please cite this article in press as: B.W. Xiong, Y.Y. Wang, Nuclear chiral doublet bands data tables, Atomic Data and Nuclear Data Tables (2018), https://doi.org/10.1016/j.adt.2018.05.002.

Table 1 (*continued*)

Nuclei	$I^{\pi}(\hbar)$	E (keV)		$B(M1)/B(E2)$ (μ_N^2/e^2b^2)		References
		yrast	side	yrast	side	
	13^+	1173*	1387	8.3	1.2	
	14^+	1544*	1744	0.8	6.9	
	15^+	2009*	2188	3.7	4.9	
	16^+	2419*	2647			
	17^+	2913*	3100	2.6	2.2	
	18^+	3349*				
	19^+	3864*				
	20^+	4336*				
$^{130}_{55}Cs_{75}$	10^+	959.7*				[24,86,93,129–131]
	11^+	1312.7*	1506.4			
	12^+	1602.4*	1907.7	$4.12\ (^{+1.77}_{-1.39})$		
	13^+	2019.0*	2280.7	$6.75\ (^{+2.18}_{-2.26})$	$2.13\ (^{+1.41}_{-1.02})$	
	14^+	2445.1*	2632.0	$1.71\ (^{+0.94}_{-0.70})$	$2.50\ (^{+0.67}_{-1.35})$	
	15^+	2913.5*	3085.0	$4.84\ (^{+3.99}_{-2.93})$	$7.84\ (^{+7.70}_{-4.91})$	
	16^+	3379.1*	3563.4	$1.00\ (^{+0.24}_{-0.24})$		
	17^+	3871.0*	4038.4	$5.66\ (^{+4.53}_{-3.24})$	4.04	
	18^+	4320.8		3.25		
	19^+	4859.0	5105.1			
	20^+	5338.4				
	21^+	5899.3				
	22^+	6450.3				
	23^+	6930.6				
	24^+	7487.5				
	26^+	8622.0				
$^{132}_{55}Cs_{77}$	9^+	1131				[24,94,132]
	10^+	1282	1729			
	11^+	1683	1891			
	12^+	1982	2202	$1.3\ (^{+0.2}_{-0.2})$		
	13^+	2410	2515	$5.9\ (^{+1.0}_{-1.0})$		
	14^+	2865	2894	$1.4\ (^{+0.3}_{-0.3})$		
	15^+	3311		$6.1\ (^{+0.7}_{-0.7})$		
	16^+	3789		$2.2\ (^{+0.6}_{-0.6})$		
	17^+	4241		$3.1\ (^{+0.6}_{-0.6})$		
	18^+	4665		$4.0\ (^{+1.4}_{-1.4})$		
	19^+	5074				
$^{128}_{57}La_{71}$	8^+	0.0*				[95]
	9^+	104.0*				
	10^+	242.5*		$1.87487\ (^{+0.37497}_{-0.37497})$		
	11^+	477.7*	808.2	$2.27708\ (^{+0.45542}_{-0.45542})$		
	12^+	700.0*	1078.7	$2.03719\ (^{+0.40744}_{-0.40744})$		
	13^+	1035.0*	1465.8	$2.39101\ (^{+0.47820}_{-0.47820})$	$1.38023\ (^{+0.82814}_{-0.82814})$	
	14^+	1334.0*	1778.1	$1.76221\ (^{+0.35244}_{-0.35244})$	$1.64005\ (^{+0.98403}_{-0.98403})$	
	15^+	1752.6*	2209.9	$1.97941\ (^{+0.39588}_{-0.39588})$	$1.50467\ (^{+0.90280}_{-0.90280})$	
	16^+	2121.0*	2580.3	$1.60661\ (^{+0.32132}_{-0.32132})$	$2.16842\ (^{+1.30105}_{-1.30105})$	
	17^+	2611.4*	3129.4	$1.25884\ (^{+0.50354}_{-0.50354})$		
	18^+	3044.2*	3551.3	$1.23285\ (^{+0.49314}_{-0.49314})$		
	19^+	3592.9*	4144.4	$1.32745\ (^{+0.51771}_{-0.51771})$		
	20^+	4090.1*	4593.3			
	21^+	4679.9*				
	22^+	5243.4				
	23^+	5855.3				
	24^+	6486.4				
$^{130}_{57}La_{73}$	9	0				[96]
	10	138				
	11	417	693			
	12	663	1050			
	13	1037	1393			
	14	1363*	1778			
	15	1809*	2204			
	16	2202*	2576			
	17	2712*				
	18	3157*				

(*continued on next page*)

Please cite this article in press as: B.W. Xiong, Y.Y. Wang, Nuclear chiral doublet bands data tables, Atomic Data and Nuclear Data Tables (2018), https://doi.org/10.1016/j.adt.2018.05.002.

Table 1 (*continued*)

Nuclei	$I^{\pi}(\hbar)$	E (keV)		$B(M1)/B(E2)$ (μ_N^2/e^2b^2)		References
		yrast	side	yrast	side	
	20	4208*				
$^{132}_{57}La_{75}$	10^+	936.4*				[23,86,92,97,129]
	11^+	1229.4*	1558.4			
	12^+	1523.4*	1919.4	$7.8\,(^{+0.4}_{-0.4})$		
	13^+	1915.4*	2299.4	$7.5\,(^{+0.4}_{-0.4})$		
	14^+	2300.4*	2703.4	$5.7\,(^{+0.1}_{-0.1})$		
	15^+	2753.4*	3130.4	$5.7\,(^{+0.2}_{-0.2})$		
	16^+	3205.4*		$5.2\,(^{+0.2}_{-0.2})$		
	17^+	3712.4*		$6.8\,(^{+0.4}_{-0.4})$		
	18^+	4199.4*		$4.9\,(^{+0.3}_{-0.3})$		
	19^+	4758.4*		$3.4\,(^{+0.4}_{-0.4})$		
	20^+	5218.4*				
	22^+	6337.4				
$^{133}_{57}La_{76}$	7.5^+	2290				[98]
	8.5^+	2367				
	9.5^+	2502	2726	$5.7\,(^{+3.3}_{-3.3})$		
	10.5^+	2681	2893	$20.0\,(^{+10.0}_{-10.0})$		
	11.5^+	2927	3110	$6.7\,(^{+1.7}_{-1.7})$	$4.2543\,(^{+1.2181}_{-1.2181})$	
	12.5^+	3258	3382	$4.7\,(^{+1.1}_{-1.1})$	$3.78366\,(^{+2.32055}_{-2.32055})$	
	13.5^+	3614	3778	$7.3\,(^{+0.7}_{-0.7})$	$4.7\,(^{+2.2}_{-2.2})$	
	14.5^+	4030	4134	$18.4\,(^{+5.0}_{-5.0})$	$10.5\,(^{+4.0}_{-4.0})$	
	15.5^+	4475		$5.8\,(^{+1.0}_{-1.0})$		
	16.5^+	4906		$3.0\,(^{+2.0}_{-2.0})$		
	17.5^+	5352		$2.0\,(^{+1.2}_{-1.2})$		
	19.5^+	6283				
$^{134}_{57}La_{77}$	10^+	813*				[99]
	11^+	1195*	1412			
	12^+	1533*	1710	$3.6\,(^{+0.2}_{-0.2})$		
	13^+	1969*	2051	$12.6\,(^{+0.6}_{-0.6})$		
	14^+	2404	2418	$3.4\,(^{+0.2}_{-0.2})$		
	15^+	2849		$10.3\,(^{+0.6}_{-0.6})$		
	16^+	3284		$10.0\,(^{+0.8}_{-0.8})$		
	17^+	3775*		$10.1\,(^{+0.7}_{-0.7})$		
	18^+	4120*		$1.1\,(^{+0.1}_{-0.1})$		
	19^+	4698*		$8.0\,(^{+0.7}_{-0.7})$		
	20^+	5079*		$1.0\,(^{+0.2}_{-0.2})$		
	21^+	5714		$4.6\,(^{+0.3}_{-0.3})$		
	22^+	6137*				
	23^+	6741*				
	24^+	7179*				
$^{133}_{58}Ce_{75}$	8.5^+	2249				[53]
	9.5^+	2379	2465			
	10.5^+	2585	2706			
	11.5^+	2809	2922	$9.711\,(^{+0.153}_{-0.153})$		
	12.5^+	3093	3199	$9.522\,(^{+0.134}_{-0.134})$	$9.393\,(^{+0.102}_{-0.102})$	
	13.5^+	3399	3534	$9.621\,(^{+0.142}_{-0.142})$	$9.834\,(^{+0.191}_{-0.191})$	
	14.5^+	3745	3933	$9.471\,(^{+0.136}_{-0.136})$	$9.337\,(^{+0.143}_{-0.143})$	
	15.5^+	4177	4334	$9.591\,(^{+0.127}_{-0.127})$	$9.459\,(^{+0.154}_{-0.154})$	
	16.5^+	4623	4775	$9.428\,(^{+0.143}_{-0.143})$	$9.435\,(^{+0.152}_{-0.152})$	
	11.5^-	3198				[53]
	12.5^-	3338				
	13.5^-	3493				
	14.5^-	3733	4162			

(*continued on next page*)

Please cite this article in press as: B.W. Xiong, Y.Y. Wang, Nuclear chiral doublet bands data tables, Atomic Data and Nuclear Data Tables (2018), https://doi.org/10.1016/j.adt.2018.05.002.

Table 1 (*continued*)

Nuclei	$I^{\pi}(\hbar)$	E (keV)		$B(M1)/B(E2)$ (μ_N^2/e^2b^2)		References
		yrast	side	yrast	side	
	15.5^-	4028	4445	11.8286 $(^{+0.1243}_{-0.1243})$		
	16.5^-	4370	4808	11.2305 $(^{+0.2352}_{-0.2352})$		
	17.5^-	4761	5175	11.6328 $(^{+0.1235}_{-0.1235})$	10.8364 $(^{+0.1235}_{-0.1235})$	
	18.5^-	5177	5617	11.0246 $(^{+0.1253}_{-0.1253})$	10.4323 $(^{+0.1253}_{-0.1253})$	
	19.5^-	5632	6040	10.9486 $(^{+0.2104}_{-0.2104})$	10.5896 $(^{+0.2104}_{-0.2104})$	
	20.5^-	6112	6508	10.9207 $(^{+0.1345}_{-0.1345})$	10.3983 $(^{+0.1345}_{-0.1345})$	
	21.5^-	6624	6999	10.6351 $(^{+0.1423}_{-0.1423})$	10.4571 $(^{+0.1423}_{-0.1423})$	
	22.5^-	7167	7557	10.7351 $(^{+0.2134}_{-0.2134})$	10.2723 $(^{+0.2134}_{-0.2134})$	
	23.5^-	7739		10.4997 $(^{+0.2365}_{-0.2365})$		
	24.5^-	8339				
$^{132}_{59}Pr_{73}$	9	0				[96,133]
	10	131*		3.3 $(^{+0.5}_{-0.5})$		
	11	397*	727	2.3 $(^{+0.3}_{-0.3})$		
	12	638*	1033	2.5 $(^{+0.3}_{-0.3})$		
	13	1021*	1458	2.6 $(^{+0.3}_{-0.3})$		
	14	1342*	1827	1.7 $(^{+0.2}_{-0.2})$		
	15	1795*		2.4 $(^{+0.1}_{-0.1})$		
	16	2190*		1.6 $(^{+0.5}_{-0.5})$		
	17	2675		2.0 $(^{+1.0}_{-1.0})$		
	18	3133*		1.3 $(^{+0.3}_{-0.3})$		
	19	3608		1.6 $(^{+0.5}_{-0.5})$		
$^{134}_{59}Pr_{75}$	9^+	559	797			[26,86,100,129,134–137]
	10^+	764	931			
	11^+	930	1142			
	12^+	1213	1409			
	13^+	1537*	1659	35.22 $(^{+0.11}_{-0.11})$		
	14^+	1874	2017	150.52 $(^{+0.43}_{-0.43})$		
	15^+	2243*	2456	37.11 $(^{+0.12}_{-0.12})$	7.42 $(^{+0.02}_{-0.02})$	
	16^+	2643	2901	7.89 $(^{+0.02}_{-0.02})$	7.93 $(^{+0.02}_{-0.02})$	
	17^+	3115	3347	8.59 $(^{+0.02}_{-0.02})$	10.97 $(^{+0.04}_{-0.04})$	
	18^+	3582	3858	4.20 $(^{+0.01}_{-0.01})$	9.78 $(^{+0.03}_{-0.03})$	
	19^+	4172	4338	3.08 $(^{+0.01}_{-0.01})$	9.04 $(^{+0.04}_{-0.04})$	
	20^+	4648		2.12 $(^{+0.01}_{-0.01})$		
	21^+	5343		4.57 $(^{+0.01}_{-0.01})$		
	22^+	5839				
	23^+	6534				
$^{135}_{60}Nd_{75}$	11.5^-	2819.4				[38,138]
	12.5^-	2940.4				
	13.5^-	3110.5	3607.4			
	14.5^-	3358.2*	3780.4	10.00 $(^{+2.26}_{-2.26})$		
	15.5^-	3649.5*	4006.4	7.81 $(^{+1.35}_{-1.35})$	9.64 $(^{+1.30}_{-1.30})$	
	16.5^-	4007.7*	4288.4	6.88 $(^{+2.30}_{-2.30})$	7.50 $(^{+2.11}_{-2.11})$	
	17.5^-	4413.7*	4597.4	7.50 $(^{+1.33}_{-1.33})$	7.86 $(^{+2.61}_{-2.61})$	
	18.5^-	4852.7*	4969.4	5.31 $(^{+1.31}_{-1.31})$	5.86 $(^{+2.23}_{-2.23})$	
	19.5^-	5315.7*	5409.4	16.15 $(^{+0.82}_{-0.82})$	17.27 $(^{+0.73}_{-0.73})$	
	20.5^-	5787.7*	5921.4	11.05 $(^{+0.94}_{-0.94})$		
	21.5^-	6281.7*		9.52 $(^{+1.13}_{-1.13})$		
	22.5^-	6799.7				
$^{136}_{60}Nd_{76}$	11^+	4445				[56]
	12^+	4665				
	13^+	4919				
	14^+	5213				
	15^+	5558	5635	4.0 $(^{+1.3}_{-1.3})$		
	16^+	5969	6053	31 $(^{+17}_{-17})$		
	17^+	6423	6485	7.0 $(^{+4.8}_{-4.8})$		
	18^+	6908	6989			

(*continued on next page*)

Please cite this article in press as: B.W. Xiong, Y.Y. Wang, Nuclear chiral doublet bands data tables, Atomic Data and Nuclear Data Tables (2018), https://doi.org/10.1016/j.adt.2018.05.002.

Table 1 (*continued*)

Nuclei	$I^{\pi}(\hbar)$	E (keV)		$B(M1)/B(E2)$ (μ_N^2/e^2b^2)		References
		yrast	side	yrast	side	
	19^+	7502	7468			
	20^+	8115				
	15^+	6229				[56]
	16^+	6347				
	17^+	6578		38		
	18^+	6883		14		
	19^+	7292		39.7		
	20^+	7668		$93\ (^{+28}_{-28})$		
	21^+	8049	8412	453.2		
	22^+	8465	8838	197.7		
	23^+	8946	9247	115		
	24^+	9489	9694			
	25^+	10089	10204			
	26^+	10761	10657			
	27^+		11256			
	13^-	5348				[56]
	14^-	5531				
	15^-	5731		$7.37\ (^{+1.72}_{-1.83})$		
	16^-	5980		$3.73\ (^{+1.59}_{-1.60})$		
	17^-	6325		$11.00\ (^{+1.49}_{-1.50})$		
	18^-	6759				
	19^-	7225	7270			
	20^-	7720	7721	$54.30\ (^{+23.20}_{-24.63})$		
	21^-	8169	8214	$41.84\ (^{+9.15}_{-9.27})$		
	22^-	8689	8751			
	23^-	9231				
	24^-	9786		$8.69\ (^{+5.05}_{-5.06})$		
	14^-	5418				[56,139,140]
	15^-	5648				
	16^-	5957		$7.51\ (^{+1.52}_{-1.54})$		
	17^-	6314		$14.93\ (^{+1.49}_{-1.62})$		
	18^-	6703		$20.13\ (^{+4.07}_{-4.23})$		
	19^-	7139	7259	$48.43\ (^{+9.08}_{-8.92})$		
	20^-	7566	7725	$43.19\ (^{+11.42}_{-11.75})$		
	21^-	8011	8199	$34.79\ (^{+5.48}_{-4.92})$		
	22^-	8499	8616	$18.65\ (^{+2.03}_{-2.20})$		
	23^-	9009	9080	$5.94\ (^{+3.21}_{-3.27})$		
	24^-	9559	9671	$3.20\ (^{+0.96}_{-0.96})$		
	25^-	10190				
	15^+	5826				[56]
	16^+	6006				
	17^+	6238*		$4.00\ (^{+2.00}_{-2.00})$		
	18^+	6522	6932	$17.36\ (^{+9.00}_{-9.00})$		
	19^+	6867*	7213	$7.57\ (^{+0.97}_{-0.97})$		
	20^+	7255*	7543	$7.87\ (^{+2.10}_{-2.10})$	$3.22\ (^{+2.00}_{-2.04})$	
	21^+	7685*	7927	$5.63\ (^{+0.75}_{-0.79})$	$7.04\ (^{+2.98}_{-3.07})$	
	22^+	8148*	8355	$6.35\ (^{+0.76}_{-0.74})$	$7.67\ (^{+4.70}_{-5.08})$	
	23^+	8652*	8828	$6.48\ (^{+1.30}_{-1.30})$	$6.46\ (^{+2.92}_{-2.98})$	
	24^+	9178*	9347	$6.60\ (^{+3.00}_{-3.00})$	$5.98\ (^{+4.03}_{-0.17})$	
	25^+	9745*	9911	$3.70\ (^{+2.00}_{-2.00})$		
	26^+	10345*	10504	$2.69\ (^{+1.90}_{-1.90})$		
	27^+	10967*	11117			
	28^+	11651*				
	29^+	12335*				
$^{137}_{60}Nd_{77}$	13.5^-	3895				[101]
	14.5^-	4159				
	15.5^-	4513	4821	15.1		

(*continued on next page*)

Table 1 (*continued*)

Nuclei	$I^{\pi}(\hbar)$	E (keV)		$B(M1)/B(E2)$ (μ_N^2/e^2b^2)		References
		yrast	side	yrast	side	
	16.5^-	4909*	5107	$13.7\,(^{+4.9}_{-4.9})$		
	17.5^-	5372*	5415	$21.7\,(^{+6.5}_{-6.5})$		
	18.5^-	5812	5787*	$39.2\,(^{+15.7}_{-15.7})$		
	19.5^-	6193	6262	$20.9\,(^{+6.8}_{-6.8})$		
	20.5^-	6668*	6794	$9.0\,(^{+4.7}_{-4.7})$		
	21.5^-	7099*	7313	$5.8\,(^{+2.1}_{-2.1})$		
	22.5^-	7650*	7701	$5.7\,(^{+3.4}_{-3.4})$		
	23.5^-	8347	8196	$9.4\,(^{+5.6}_{-5.6})$		
	24.5^-		8744			
	25.5^-		9336*			
$^{138}_{60}Nd_{78}$	10^+		4344			[30,63]
	11^+	4381	4546			
	12^+	4737	4779			
	13^+		5069			
	14^+		5363			
	15^+		5678			
	16^+		6179			
	17^+		6760			
	13^-	5493				[63]
	14^-	5577				
	15^-	5770	6018	6.5		
	16^-	6001	6285	14.1		
	17^-	6287	6560	11.2		
	18^-	6668	6909	31.6		
	19^-	7047*	7415	51.9		
	20^-	7564		48.5		
	21^-	8013*		42.9		
$^{136}_{61}Pm_{75}$	8^+	0*				[86,102,104,129,141,142]
	9^+	99*				
	10^+	267*				
	11^+	552*	858	$9.8\,(^{+4.3}_{-4.3})$		
	12^+	844*	1146	$5.5\,(^{+0.7}_{-0.7})$		
	13^+	1252*	1510	$5.1\,(^{+0.7}_{-0.7})$	$6.1\,(^{+1.7}_{-1.7})$	
	14^+	1608*	1936	$2.6\,(^{+0.3}_{-0.3})$	$5.7\,(^{+1.5}_{-1.5})$	
	15^+	2086*	2360	$3.8\,(^{+0.9}_{-0.9})$		
	16^+	2504*	2819	$1.0\,(^{+0.4}_{-0.4})$		
	17^+	3010*	3254	$1.8\,(^{+0.6}_{-0.6})$		
	18^+	3479*	3654	$2.1\,(^{+3.6}_{-3.6})$		
	19^+	3935*	4088			
	20^+	4377*	4469			
	21^+	4814*	4872			
$^{138}_{61}Pm_{77}$	9^+	585*				[103]
	10^+	706*				
	11^+	1063*	1319			
	12^+	1413*	1619	$3.46\,(^{+0.38}_{-0.38})$		
	13^+	1890*	2097	$3.81\,(^{+0.34}_{-0.34})$	$3.2\,(^{+0.5}_{-0.5})$	
	14^+	2283*	2506	$2.90\,(^{+0.38}_{-0.38})$	$2.4\,(^{+0.5}_{-0.5})$	
	15^+	2829*	3077	$2.35\,(^{+0.33}_{-0.33})$	$2.5\,(^{+0.9}_{-0.9})$	
	16^+	3279		$1.74\,(^{+0.40}_{-0.40})$		
	17^+	3855		$1.83\,(^{+0.55}_{-0.55})$		
	18^+	4340				
$^{138}_{63}Eu_{75}$	8^+	0				[104,141,142]
	9^+	104*				
	10^+	271*	628			
	11^+	544*	792	$3.1\,(^{+0.4}_{-0.4})$		
	12^+	806*	1091	$2.3\,(^{+0.1}_{-0.1})$	$3.1\,(^{+0.2}_{-0.2})$	
	13^+	1168*	1442	$2.5\,(^{+0.3}_{-0.3})$	$4.0\,(^{+1.0}_{-1.0})$	
	14^+	1488*	1847	$1.6\,(^{+0.2}_{-0.2})$		
	15^+	1916*	2230	$2.1\,(^{+0.6}_{-0.6})$		
	16^+	2298*	2708	$1.3\,(^{+0.2}_{-0.2})$		
	17^+	2761*	3128	$2.2\,(^{+0.5}_{-0.5})$		
	18^+	3177*		$1.4\,(^{+0.4}_{-0.4})$		
	19^+	3589*		$3.4\,(^{+0.9}_{-0.9})$		
	20^+	4015*		$3.4\,(^{+0.7}_{-0.7})$		
	21^+	4456*		$3.8\,(^{+0.7}_{-0.7})$		

(*continued on next page*)

Please cite this article in press as: B.W. Xiong, Y.Y. Wang, Nuclear chiral doublet bands data tables, Atomic Data and Nuclear Data Tables (2018), https://doi.org/10.1016/j.adt.2018.05.002.

Table 1 (*continued*)

Nuclei	$I^{\pi}(\hbar)$	E (keV)		$B(M1)/B(E2)$ (μ_N^2/e^2b^2)		References
		yrast	side	yrast	side	
	22^+	4982*		1.7 $(^{+0.8}_{-0.8})$		
	23^+	5486				
	24^+	6025*				
	25^+	6632*				
$^{140}_{63}Eu_{77}$	5^-	0.0*				[105,142]
	6^-	170.6*	285.4			
	7^-	361.7*		0.94 $(^{+0.17}_{-0.17})$		
	8^-	654.6	763.1	0.00 $(^{+0.08}_{-0.08})$		
	9^-	898.6		0.41 $(^{+0.31}_{-0.31})$		
	10^-	1376.6	1364.8			
	11^-	1614.2				
	12^-	1959.6	2197.1			
	13^-	2444.2	2427.5			
	14^-	2884.6	2597.5			
	15^-		2970.4			
	16^-		3424.4			
	17^-		3884.4			
	18^-		4264.0			
	8^+		53.0			[105,142]
	9^+	0.0	147.9			
	10^+	71.0				
	11^+	436.8	554.5			
	12^+	711.5		0.40 $(^{+0.11}_{-0.11})$		
	13^+	1157.5	1201.9	3.42 $(^{+0.90}_{-0.90})$		
	14^+	1518.8		1.53 $(^{+0.89}_{-0.89})$		
	15^+	1989.3	2020.9	1.97 $(^{+0.39}_{-0.39})$		
	16^+	2438.8				
	17^+	2500.2	2636.9			
	19^+	3147.9				
	21^+	3902.1				
	23^+	4809.5				
	25^+	5801.2				
$^{188}_{77}Ir_{111}$	9^-	923.7*				[106]
	10^-	1222.3*				
	11^-	1398.9*		0.90 $(^{+0.04}_{-0.04})$		
	12^-	1711.2*		1.80 $(^{+0.05}_{-0.05})$		
	13^-	1922.8*	2168.2	0.64 $(^{+0.03}_{-0.03})$		
	14^-	2290.1*	2443.6	1.13 $(^{+0.05}_{-0.05})$		
	15^-	2556.7*	2679.7	0.58 $(^{+0.03}_{-0.03})$	1.25 $(^{+0.12}_{-0.12})$	
	16^-	2990.5	2945.3	0.77 $(^{+0.06}_{-0.06})$	1.28 $(^{+0.18}_{-0.18})$	
	17^-		3201.7			
$^{193}_{81}Tl_{112}$	13.5^-	3092				[107]
	14.5^-	3251	3402			
	15.5^-	3402	3684			
	16.5^-	3624	3883			
	17.5^-	3862	4253			
	18.5^-	4188	4505			
	19.5^-	4525	4874			
	20.5^-	4868	5230			
$^{194}_{81}Tl_{113}$	8^-	293				[108,143,144]
	9^-	338				
	10^-	434				
	11^-	712	1175			
	12^-	957	1481			
	13^-	1361	1738			
	14^-	1644	2001			
	15^-	2112	2344			
	16^-	2404	2682			
	17^-	2882	3003			
	18^-	3130	3257			
	19^-	3381	3427			
	20^-	3518	3628			
	21^-	3840	3877	4.45 $(^{+2.92}_{-1.83})$		
	22^-	4081	4181	2.46 $(^{+1.39}_{-0.77})$	6.17 $(^{+5.01}_{-2.34})$	
	23^-	4462	4560	7.18 $(^{+5.89}_{-2.61})$	4.03	
	24^-	4824		3.66 $(^{+3.61}_{-2.06})$		
$^{198}_{81}Tl_{117}$	8^-	391				[109,145]
	9^-	463				
	10^-	585	1111			

(*continued on next page*)

Please cite this article in press as: B.W. Xiong, Y.Y. Wang, Nuclear chiral doublet bands data tables, Atomic Data and Nuclear Data Tables (2018), https://doi.org/10.1016/j.adt.2018.05.002.

Table 1 (*continued*)

Nuclei	$I^{\pi}(\hbar)$	E (keV)		$B(M1)/B(E2)$ (μ_N^2/e^2b^2)		References
		yrast	side	yrast	side	
	11^-	844*	1293	$3.8\,(^{+0.4}_{-0.4})$		
	12^-	1091*	1541	$4.1\,(^{+0.5}_{-0.5})$		
	13^-	1493*	1857	$3.9\,(^{+0.5}_{-0.5})$	$4.4\,(^{+1.4}_{-1.4})$	
	14^-	1790*	2294	$3.1\,(^{+0.6}_{-0.6})$	$2.5\,(^{+1.2}_{-1.2})$	
	15^-	2278		$4.3\,(^{+0.9}_{-0.9})$		
	16^-	2552		$6.4\,(^{+2.1}_{-2.1})$		
	17^-	2947		$1.7\,(^{+0.8}_{-0.8})$		
	18^-	3219				

Please cite this article in press as: B.W. Xiong, Y.Y. Wang, Nuclear chiral doublet bands data tables, Atomic Data and Nuclear Data Tables (2018), https://doi.org/10.1016/j.adt.2018.05.002.

Table 2
Chiral doublet bands with $B(M1)$ and $B(E2)$ values. See Explanation of Tables for details.

Nuclei	I^π ($\hbar$)	E (keV)		$B(M1)$ (μ_N^2)		$B(E2)$ (e^2b^2)		References
		yrast	side	yrast	side	yrast	side	
$^{103}_{45}Rh_{58}$	10.5^+	3238						[54,117,118]
	11.5^+	3357						
	12.5^+	3591						
	13.5^+	3899	4445					
	14.5^+	4281	4789					
	15.5^+	4665	5166					
	16.5^+	5156	5616					
	17.5^+	5622	6062					
	18.5^+	6163	6528					
	19.5^+	6706	7074					
	20.5^+	7317						
	21.5^+	7952						
	6.5^-	2033						[54,117,118]
	7.5^-	2219						
	8.5^-	2343						
	9.5^-	2538	2744					
	10.5^-	2751	2934					
	11.5^-	3011*	3273					
	12.5^-	3327*	3615	$2.3\,(^{+0.4}_{-0.4})$		$0.077\,(^{+0.014}_{-0.014})$		
	13.5^-	3769*	4080	$1.8\,(^{+0.2}_{-0.2})$		$0.14\,(^{+0.03}_{-0.03})$		
	14.5^-	4195	4559	$1.2\,(^{+0.4}_{-0.4})$		$0.11\,(^{+0.04}_{-0.04})$		
	15.5^-	4763	5091					
	16.5^-	5297	5685					
	17.5^-	5923						
	18.5^-	6586						
	19.5^-	7186						
	6.5^-	2228						[54,117,118]
	7.5^-	2366	2443					
	8.5^-	2520	2643					
	9.5^-	2699	2871					
	10.5^-	2915	3090					
	11.5^-	3227	3416					
	12.5^-	3668	3778					
	13.5^-	4106	4210					
	14.5^-	4606	4659					
	15.5^-	5061	5059					
	16.5^-	5577						
	17.5^-	6143						
$^{104}_{45}Rh_{59}$	9^-	483*		$2.3\,(^{+0.2}_{-0.2})$				[80,118]
	10^-	840*	1228	$0.95\,(^{+0.08}_{-0.08})$		$0.063\,(^{+0.017}_{-0.017})$		
	11^-	1168*	1582	$0.91\,(^{+0.12}_{-0.12})$		$0.093\,(^{+0.020}_{-0.020})$		
	12^-	1636*	1971	$0.44\,(^{+0.06}_{-0.06})$		$0.039\,(^{+0.010}_{-0.010})$		
	13^-	2111*	2370	$0.42\,(^{+0.15}_{-0.15})$		$0.067\,(^{+0.025}_{-0.025})$		
	14^-	2639*	2834					
	15^-	3229*	3320					
	16^-	3800*	3876					
	17^-	4406	4406					
$^{106}_{47}Ag_{59}$	10^-	2271.7	3203.8					[85,120–124]
	11^-	2441.4	3423.5					
	12^-	2660.4	3676.0					
	13^-	2930.2	3941.6					
	14^-	3256.7	4263.7	$1.335\,(^{+0.397}_{-0.397})$		$0.100\,(^{+0.043}_{-0.043})$		
	15^-	3686.1	4636.6	$0.968\,(^{+0.211}_{-0.211})$	$3.164\,(^{+0.873}_{-0.873})$	$0.106\,(^{+0.020}_{-0.020})$	$0.271\,(^{+0.084}_{-0.084})$	
	16^-	4223.3*	5051.7	$0.539\,(^{+0.096}_{-0.096})$	$2.041\,(^{+0.317}_{-0.317})$	$0.099\,(^{+0.015}_{-0.015})$	$0.232\,(^{+0.050}_{-0.050})$	
	17^-	4742.6*	5561.2	$0.463\,(^{+0.010}_{-0.010})$	$1.050\,(^{+0.221}_{-0.221})$	$0.101\,(^{+0.019}_{-0.019})$	$0.153\,(^{+0.039}_{-0.039})$	
	18^-	5414.9*	6065.8	$0.635\,(^{+0.251}_{-0.251})$	$1.291\,(^{+0.327}_{-0.327})$	$0.085\,(^{+0.032}_{-0.032})$	$0.202\,(^{+0.043}_{-0.043})$	
	19^-	6026.8*	6691.0	$0.290\,(^{+0.054}_{-0.054})$	$0.739\,(^{+0.202}_{-0.202})$	$0.051\,(^{+0.009}_{-0.009})$	$0.136\,(^{+0.034}_{-0.034})$	
	20^-	6760.7*	7276.7	$0.289\,(^{+0.072}_{-0.072})$	$0.517\,(^{+0.167}_{-0.167})$	$0.043\,(^{+0.011}_{-0.011})$	$0.079\,(^{+0.026}_{-0.026})$	
	21^-	7531.7	7945.6	$0.065\,(^{+0.028}_{-0.028})$		$0.035\,(^{+0.014}_{-0.014})$		
	22^-	8192.5				$0.047\,(^{+0.010}_{-0.010})$		
$^{107}_{47}Ag_{60}$	10.5^-	2620.8*	2901.6					[60,125,126]
	11.5^-	2928.7*	3091.8	$1.25\,(^{+0.36}_{-0.36})$		$0.18\,(^{+0.06}_{-0.06})$		
	12.5^-	3338.7*	3392.0	$0.82\,(^{+0.18}_{-0.18})$		$0.09\,(^{+0.02}_{-0.02})$		
	13.5^-	3800.0	3897.5	$0.85\,(^{+0.17}_{-0.17})$		$0.08\,(^{+0.02}_{-0.02})$		
	14.5^-	4270.0	4349.6	> 0.39		> 0.06		
	15.5^-	4878.8	4932.0					
	16.5^-	5437.3						
	11.5^+	3334.8						[60,125,126]
	12.5^+	3556.7		$5.2\,(^{+2.3}_{-2.3})$		$0.15\,(^{+0.07}_{-0.07})$		

(*continued on next page*)

Please cite this article in press as: B.W. Xiong, Y.Y. Wang, Nuclear chiral doublet bands data tables, Atomic Data and Nuclear Data Tables (2018), https://doi.org/10.1016/j.adt.2018.05.002.

Table 2 (*continued*)

Nuclei	I^π ($\hbar$)	E (keV)		$B(M1)$ (μ_N^2)		$B(E2)$ (e^2b^2)		References
		yrast	side	yrast	side	yrast	side	
	13.5^+	3851.3		$2.7\,(^{+0.6}_{-0.6})$		$0.23\,(^{+0.05}_{-0.05})$		
	14.5^+	4230.0*	4841.7	$1.8\,(^{+0.3}_{-0.3})$		$0.15\,(^{+0.03}_{-0.03})$		
	15.5^+	4626.4*	5131.1	$1.9\,(^{+0.3}_{-0.3})$		$0.14\,(^{+0.03}_{-0.03})$		
	16.5^+	5120.5*	5448.9	$1.9\,(^{+0.4}_{-0.4})$		$0.23\,(^{+0.06}_{-0.06})$		
	17.5^+	5621.5*	5818.4	> 1.25		> 0.16		
	18.5^+	6192.8*	6250.2					
	19.5^+	6785.9	6761.3*					
	20.5^+	7441.1	7315.5*					
	21.5^+		7919.9*					
	22.5^+		8591.2*					
$^{124}_{55}Cs_{69}$	8^+	561.9*						[90]
	9^+	619.9*						
	10^+	743.9*						
	11^+	1055.9*	1260.2					
	12^+	1275.9*	1631.2					
	13^+	1673.9*	1893.2					
	14^+	1989.9*	2265.2	$0.27\,(^{+0.05}_{-0.07})$	$0.16\,(^{+0.05}_{-0.05})$	$0.31\,(^{+0.06}_{-0.08})$	$0.12\,(^{+0.03}_{-0.04})$	
	15^+	2446.9*	2666.2	$0.41\,(^{+0.09}_{-0.13})$	$0.66\,(^{+0.16}_{-0.14})$	$0.12\,(^{+0.03}_{-0.04})$	$0.25\,(^{+0.07}_{-0.06})$	
	16^+	2858.9*	3090.2	≤ 0.05	≤ 0.05	$0.24\,(^{+0.06}_{-0.06})$	$0.13\,(^{+0.05}_{-0.05})$	
	17^+	3344.9*	3574.2	$0.41\,(^{+0.11}_{-0.07})$	$0.34\,(^{+0.11}_{-0.09})$	$0.14\,(^{+0.04}_{-0.03})$	$0.21\,(^{+0.07}_{-0.06})$	
	18^+	3832.9*		≤ 0.05		$0.19\,(^{+0.04}_{-0.04})$		
	19^+	4342.9*		$0.47\,(^{+0.07}_{-0.09})$		$0.15\,(^{+0.03}_{-0.03})$		
	20^+	4906.9*		≤ 0.05		$0.19\,(^{+0.05}_{-0.05})$		
	21^+	5424.9*		$0.38\,(^{+0.16}_{-0.09})$		$0.15\,(^{+0.04}_{-0.06})$		
	22^+	6086.9*		≤ 0.02		$0.06\,(^{+0.01}_{-0.01})$		
	23^+	6550.9		$0.16\,(^{+0.04}_{-0.04})$		$0.07\,(^{+0.01}_{-0.01})$		
	24^+	7357.9						
	25^+	7649.9						
$^{126}_{55}Cs_{71}$	9^+	0						[91,127,128]
	10^+	140						
	11^+	477	637					
	12^+	732	999					
	13^+	1128	1326					
	14^+	1471	1671	$0.14\,(^{+0.07}_{-0.02})$	$0.16\,(^{+0.05}_{-0.02})$	$0.23\,(^{+0.11}_{-0.03})$	$0.13\,(^{+0.05}_{-0.02})$	
	15^+	1935	2097	$0.47\,(^{+0.27}_{-0.07})$	$0.25\,(^{+0.16}_{-0.05})$	$0.11\,(^{+0.06}_{-0.02})$	$0.08\,(^{+0.05}_{-0.02})$	
	16^+	2350	2572	≤ 0.04	≤ 0.07	$0.14\,(^{+0.05}_{-0.02})$	$0.05\,(^{+0.03}_{-0.01})$	
	17^+	2846	3033	$0.23\,(^{+0.11}_{-0.04})$	$0.11\,(^{+0.05}_{-0.02})$	$0.08\,(^{+0.04}_{-0.01})$	$0.12\,(^{+0.05}_{-0.02})$	
	18^+	3311		≤ 0.07		$0.15\,(^{+0.05}_{-0.02})$		
	19^+	3839	4040	$0.34\,(^{+0.23}_{-0.07})$		$0.09\,(^{+0.06}_{-0.02})$	$0.07\,(^{+0.03}_{-0.01})$	
	20^+	4357		≤ 0.07		$0.09\,(^{+0.04}_{-0.01})$		
	21^+	4911		$0.18\,(^{+0.18}_{-0.07})$		$0.07\,(^{+0.07}_{-0.02})$		
$^{130}_{55}Cs_{75}$	10^+	959.7*						[24,86,93,129–131]
	11^+	1312.7*	1506.4					
	12^+	1602.4*	1907.7	$0.70\,(^{+0.22}_{-0.17})$		$0.17\,(^{+0.05}_{-0.04})$		
	13^+	2019.0*	2280.7	$0.54\,(^{+0.11}_{-0.12})$	$0.32\,(^{+0.15}_{-0.11})$	$0.08\,(^{+0.02}_{-0.02})$	$0.15\,(^{+0.07}_{-0.05})$	
	14^+	2445.1*	2632.0	$0.24\,(^{+0.10}_{-0.07})$	$0.20\,(^{+0.04}_{-0.04})$	$0.14\,(^{+0.05}_{-0.04})$	$0.08\,(^{+0.02}_{-0.02})$	
	15^+	2913.5*	3085.0	$0.92\,(^{+0.54}_{-0.40})$	$1.49\,(^{+1.05}_{-0.69})$	$0.19\,(^{+0.11}_{-0.08})$	$0.19\,(^{+0.13}_{-0.08})$	
	16^+	3379.1*	3563.4	$0.12\,(^{+0.02}_{-0.02})$		$0.12\,(^{+0.02}_{-0.02})$		
	17^+	3871.0*	4038.4	$1.98\,(^{+1.11}_{-0.81})$	> 1.01	$0.35\,(^{+0.20}_{-0.14})$	> 0.25	
	18^+	4320.8		> 0.39		> 0.12		
	19^+	4859.0	5105.1					
	20^+	5338.4						
	21^+	5899.3						
	22^+	6450.3						
	23^+	6930.6						
	24^+	7487.5						
	26^+	8622.0						
$^{134}_{59}Pr_{75}$	9^+	559	797					[26,86,100,129,134–137]
	10^+	764	931					
	11^+	930	1142					
	12^+	1213	1409					
	13^+	1537*	1659	$0.804\,(^{+0.090}_{-0.090})$				
	14^+	1874	2017	$0.678\,(^{+0.100}_{-0.100})$		$0.039\,(^{+0.019}_{-0.019})$		
	15^+	2243*	2456	$0.472\,(^{+0.090}_{-0.090})$		$0.089\,(^{+0.020}_{-0.020})$		
	16^+	2643	2901	$0.333\,(^{+0.075}_{-0.075})$		$0.050\,(^{+0.018}_{-0.018})$		
	17^+	3115	3347	$0.545\,(^{+0.067}_{-0.067})$		$0.047\,(^{+0.017}_{-0.017})$		
	18^+	3582	3858					

(*continued on next page*)

Please cite this article in press as: B.W. Xiong, Y.Y. Wang, Nuclear chiral doublet bands data tables, Atomic Data and Nuclear Data Tables (2018), https://doi.org/10.1016/j.adt.2018.05.002.

Table 2 (*continued*)

Nuclei	I^{π} ($\hbar$)	E (keV)		$B(M1)$ (μ_N^2)		$B(E2)$ (e^2b^2)		References
		yrast	side	yrast	side	yrast	side	
	19^+	4172	4338					
	20^+	4648						
	21^+	5343						
	22^+	5839						
	23^+	6534						
$^{135}_{60}Nd_{75}$	11.5^-	2819.4						[38,138]
	12.5^-	2940.4						
	13.5^-	3110.5	3607.4					
	14.5^-	3358.2*	3780.4	$3.2\,(^{+0.2}_{-0.2})$		$0.32\,(^{+0.02}_{-0.02})$		
	15.5^-	3649.5*	4006.4	$2.5\,(^{+0.3}_{-0.3})$	$2.7\,(^{+0.3}_{-0.3})$	$0.32\,(^{+0.03}_{-0.03})$	$0.28\,(^{+0.03}_{-0.03})$	
	16.5^-	4007.7*	4288.4	$2.2\,(^{+0.2}_{-0.2})$	$2.1\,(^{+0.2}_{-0.2})$	$0.32\,(^{+0.03}_{-0.03})$	$0.28\,(^{+0.03}_{-0.03})$	
	17.5^-	4413.7*	4597.4	$2.4\,(^{+0.3}_{-0.3})$	$2.2\,(^{+0.2}_{-0.2})$	$0.32\,(^{+0.03}_{-0.03})$	$0.28\,(^{+0.04}_{-0.04})$	
	18.5^-	4852.7*	4969.4	$1.7\,(^{+0.3}_{-0.3})$	$1.7\,(^{+0.2}_{-0.2})$	$0.32\,(^{+0.04}_{-0.04})$	$0.29\,(^{+0.04}_{-0.04})$	
	19.5^-	5315.7*	5409.4	$2.1\,(^{+0.3}_{-0.3})$	$1.9\,(^{+0.3}_{-0.3})$	$0.13\,(^{+0.03}_{-0.03})$	$0.11\,(^{+0.03}_{-0.03})$	
	20.5^-	5787.7*	5921.4	$2.1\,(^{+0.3}_{-0.3})$		$0.19\,(^{+0.03}_{-0.03})$		
	21.5^-	6281.7*		$2.0\,(^{+0.3}_{-0.3})$		$0.21\,(^{+0.04}_{-0.04})$		
	22.5^-	6799.7						
$^{194}_{81}Tl_{113}$	8^-	293						[108,143,144]
	9^-	338						
	10^-	434						
	11^-	712	1175					
	12^-	957	1481					
	13^-	1361	1738					
	14^-	1644	2001					
	15^-	2112	2344					
	16^-	2404	2682					
	17^-	2882	3003					
	18^-	3130	3257					
	19^-	3381	3427		< 1.25			
	20^-	3518	3628		< 1.61			
	21^-	3840	3877	$0.95\,(^{+0.32}_{-0.21})$	$1.31\,(^{+0.54}_{-0.30})$	$0.21\,(^{+0.12}_{-0.07})$		
	22^-	4081	4181	$0.97\,(^{+0.39}_{-0.21})$	$1.24\,(^{+0.43}_{-0.29})$	$0.39\,(^{+0.15}_{-0.09})$	$0.20\,(^{+0.15}_{-0.06})$	
	23^-	4462	4560	$0.34\,(^{+0.13}_{-0.07})$	< 0.27	$0.05\,(^{+0.03}_{-0.01})$	< 0.07	
	24^-	4824		$0.27\,(^{+0.18}_{-0.09})$		$0.07\,(^{+0.05}_{-0.03})$		

Please cite this article in press as: B.W. Xiong, Y.Y. Wang, Nuclear chiral doublet bands data tables, Atomic Data and Nuclear Data Tables (2018), https://doi.org/10.1016/j.adt.2018.05.002.